

**INFLUENCE OF B<sub>2</sub>O<sub>3</sub> ADDITIONS ON THE  
MICROSTRUCTURE OF MICA BASED GLASS – CERAMICS**

**A THESIS SUBMITTED TO  
THE GRADUATE SCHOOL OF NATURAL AND APPLIED SCIENCES  
OF  
MIDDLE EAST TECHNICAL UNIVERSITY**

**BY**

**HAKAN AYKUT**

**IN PARTIAL FULFILLMENT OF THE REQUIREMENTS  
FOR  
THE DEGREE OF MASTER OF SCIENCE  
IN  
METALLURGICAL AND MATERIALS ENGINEERING**

**APRIL 2005**

Approval of the Graduate School of Natural and Applied Sciences

---

Prof. Dr. Canan Özgen  
Director

I certify that this thesis satisfies all the requirements as a thesis for the degree of  
Master of Science

---

Prof. Dr. Tayfur Öztürk  
Head of Department

This is to certify that we have read this thesis end that in our opinion it is fully  
adequate, in scope and quality, as a thesis for the degree of Master of Science

---

Prof. Dr. Abdullah Öztürk  
Supervisor

Examining Committee Members

|                            |              |       |
|----------------------------|--------------|-------|
| Prof. Dr. Muharrem Timuçin | (METU, METE) | _____ |
| Prof. Dr. Abdullah Öztürk  | (METU, METE) | _____ |
| Prof. Dr. Yavuz Topkaya    | (METU, METE) | _____ |
| Prof. Dr. Ahmet Geveci     | (METU, METE) | _____ |
| Prof. Dr. Yusuf Orçan      | (METU, ES)   | _____ |

**I hereby declare that all information in this document has been obtained and presented in accordance with academic rules and ethical conduct. I also declare that, as required by these rules and conduct, I have fully cited and referenced all material and results that are not original to this work.**

Name, Last name :

Signature :

## **ABSTRACT**

### **INFLUENCE OF B<sub>2</sub>O<sub>3</sub> ADDITION ON THE MICROSTRUCTURE OF MICA BASED GLASS - CERAMICS**

AYKUT, Hakan

M.S. , Department of Metallurgical and Materials Engineering

Supervisor: Prof. Dr. Abdullah ÖZTÜRK

January 2005, 82 pages

Mica based glass - ceramics have been produced by subjecting the glasses in the SiO<sub>2</sub> , Al<sub>2</sub>O<sub>3</sub> , CaO , MgO, K<sub>2</sub>O , and F system to a controlled heat treatment called crystallization. TiO<sub>2</sub> was added into the batch in the amount of 1 wt% of the glass as nucleating agent. B<sub>2</sub>O<sub>3</sub> additions in the amounts of 1, 2, 4 and 8 wt% of the glass have been made in the batch to see and evaluate the effects of B<sub>2</sub>O<sub>3</sub> additions on the texture of the mica glass ceramics. Crystallization was accomplished in two steps, nucleation and crystal growth. Nucleation temperature was 650 °C. Crystal growth temperatures were 850 and 1000 °C. The time for holding the specimens at the temperatures was 8 hours.

The X-Ray diffraction analysis revealed that resultant glass ceramics possessed not only synthetic fluormica crystals called phlogopite which provide machinability, but also wollastonite crystals which provide biocompatibility. The scanning electron microscopy examinations have indicated that the amount and distribution of the crystalline phases varied as a function of  $B_2O_3$  content and heat treatment schedule applied.

Keywords: Glass ceramic,  $B_2O_3$ , mica, fluormica, machinability, wollastonite, biocompatibility.

## ÖZ

### **B<sub>2</sub>O<sub>3</sub> İLAVESİNİN MİKA BAZLI CAM SERAMİKLERİN MİKROYAPISI ÜZERİNE ETKİLERİ**

AYKUT, Hakan

Yüksek Lisans, Metalurji ve Malzeme Mühendisliği Bölümü

Tez Yöneticisi: Prof. Dr. Abdullah Öztürk

Ocak 2005, 82 sayfa

Mika bazlı cam seramikler, SiO<sub>2</sub>, Al<sub>2</sub>O<sub>3</sub>, CaO, MgO, K<sub>2</sub>O, ve F sisteminden oluşturulmuş camların kristalizasyon adı verilen kontrollü ısıl işleme tabi tutulması ile üretilmiştir. Camın ağırlıkça %1'i oranında TiO<sub>2</sub> ilavesi harmana çekirdeklendirici olarak eklenmiştir. B<sub>2</sub>O<sub>3</sub> ilavelerinin mika bazlı cam seramiğin dokusunda oluşturacağı etkileri gözlemlmek için camın ağırlıkça %1, 2, 4 ve 8'i oranında B<sub>2</sub>O<sub>3</sub> harmana eklenmiştir. Kristalleşme, çekirdek oluşumu ve kristal büyümesi olarak 2 adımda sonuçlanmıştır. Çekirdeklenme 650 °C' de, kristal büyümesi ise 850 ve 1000 °C' de gerçekleştirilmiştir. Örnekler bu sıcaklıklarda 8 saat tutulmuştur.

X-ışınları kırılım analizleri, mika bazlı cam seramiklerin, işlenebilirlik sağlayan ve filogopit olarak adlandırılan sentetik flormika kristallerinin yanında, biyolojik

bünyelere uygunluk sağlayan vollastonit kristallerini de içerdiğini ortaya koymuştur. Taramalı elektron mikroskop incelemeleri oluşan kristal fazın miktarının ve dağılımının,  $B_2O_3$  içeriğine ve uygulanan ısı işlem programına bağlı olarak değişim gösterdiğini açığa çıkarmıştır.

Anahtar kelimeler: Cam seramik,  $B_2O_3$ , mika, flormika, işlenebilirlik, vollastonit, bünyeye uygunluk.

To my family...

## **ACKNOWLEDGEMENTS**

I would like to thank my supervisor, Prof. Dr. Abdullah Öztürk for his expertise, helpful guidance, criticism, endless encouragement and tolerance throughout the research.

I wish to express sincere appreciations to, Prof. Dr. Muharrem Timuçin, Prof. Dr. Ahmet Geveci, Prof. Dr. Yavuz Topkaya, Prof. Dr. Yusuf Orçan for the participation on the author's committee.

I also want to express sincere thanks to Cengiz Tan for SEM examinations and EDX analyses and Necmi Avcı for performing XRD analysis.

I would like to thank to Miss Seda Çağırıcı for her support, encouragement and efforts.

Finally, I would like to offer my sincere thanks to my family for their constant encouragement, understanding and their endless support during my education.

## TABLE OF CONTENTS

|                        |      |
|------------------------|------|
| PLAGIARISM.....        | iii  |
| ABSTRACT.....          | iv   |
| ÖZ.....                | vi   |
| DEDICATION.....        | viii |
| ACKNOWLEDGEMENTS.....  | ix   |
| TABLE OF CONTENTS..... | x    |
| LIST OF TABLES.....    | xii  |
| LIST OF FIGURES.....   | xiii |

## CHAPTER

|  |    |
|--|----|
| 1. INTRODUCTION.....   | 1  |
| 2. THEORY.....   | 4  |
| 2.1 GENERAL.....   | 4  |
| 2.2 GLASSES AND GLASS CERAMICS.....                                | 8  |
| 2.3 MICA STRUCTURE.....  | 10 |
| 2.4 CRYSTALLIZATION OF GLASSES.....                                | 15 |
| 2.5 EFFECT OF TiO <sub>2</sub> ON GLASS-CERAMICS.....              | 17 |
| 2.6 EFFECT OF MgF <sub>2</sub> ON GLASS-CERAMICS.....              | 19 |
| 2.7 EFFECT OF B <sub>2</sub> O <sub>3</sub> ON GLASS-CERAMICS..... | 19 |
| 3. EXPERIMENTAL PROCEDURE.....                                     | 20 |
| 3.1 SAMPLE PREPARATION.....  | 20 |
| 3.1.1 Batch Materials.....   | 20 |

|   |    |
|---|----|
| 3.1.2 Formation of Glasses.....             | 21 |
| 3.1.3 Preparation of Glass-Ceramics.....    | 22 |
| 3.2 ANALYSIS.....                           | 24 |
| 3.2.1 X-Ray Diffraction.....                | 24 |
| 3.2.2 Differential Thermal Analysis.....    | 24 |
| 3.2.3 Scanning Electron Microscope.....     | 24 |
| <br>  |    |
| 4. RESULTS AND DISCUSSIONS.....             | 27 |
| 4.1 GENERAL.....                            | 27 |
| 4.1.1 Formation of Glasses.....             | 27 |
| 4.1.2 Preparation of Glass-Ceramics.....    | 30 |
| 4.2 ANALYSES.....                           | 32 |
| 4.2.1 Differential Thermal Analysis.....    | 32 |
| 4.2.2 X-Ray Diffraction.....                | 37 |
| 4.2.3 Scanning Electron Microscope.....     | 44 |
| 4.2.4 Energy Dispersive X-Ray Analysis..... | 63 |
| <br>  |    |
| 5. CONCLUSIONS.....                         | 73 |
| Recommandations For Further Studies.....    | 74 |
| REFERENCES.....                             | 75 |

## LIST OF TABLES

| TABLE |  | PAGE |
|-------|--|------|
| 3.1   | The ingredients, batch and final compositions of the glass investigated..... | 21   |

## LIST OF FIGURES

| FIGURES  | PAGE |
|--|------|
| 2.1 Clinical uses of bioceramics.....  | 5    |
| 2.2 Schematic of fluorphlogopite structure.....  | 12   |
| 2.3 Schematic of the formation of a glass ceramic.....   | 16   |
| 3.1 Schematic representation of the heat treatment applied to<br>convert the glass to glass ceramic..... | 24   |
| 3.2 Flow chart of the experimental procedure.....  | 26   |
| 4.1 The XRD pattern of the melts.....  | 28   |
| 4.2 DTA thermogram of the glass containing 1wt% of B <sub>2</sub> O <sub>3</sub> .....                   | 30   |
| 4.3 DTA thermogram without B <sub>2</sub> O <sub>3</sub> content.....                                    | 33   |
| 4.4 DTA thermogram of the glass containing 4 wt% of B <sub>2</sub> O <sub>3</sub> .....                  | 34   |

|      |   |    |
|------|---|----|
| 4.5  | DTA thermogram of the glass containing 8 wt% of B <sub>2</sub> O <sub>3</sub> .....   | 34 |
| 4.6  | DTA thermogram of a mica glass ceramic given by Kodaira....   | 36 |
| 4.7  | XRD pattern of the glass ceramic samples were heat treated at 650 °C and 850 °C.....  | 38 |
| 4.8  | XRD pattern of the glass ceramic samples were heat treated at 650 °C and 1000 °C.....   | 39 |
| 4.9  | XRD pattern of the sample containing 4 wt% of B <sub>2</sub> O <sub>3</sub> were heat treated at 650 °C and 1000 °C when the lid of the crucible was closed.....  | 40 |
| 4.10 | XRD pattern of the sample containing 8 wt% of B <sub>2</sub> O <sub>3</sub> were heat treated at 650 °C and 1000 °C when the lid of the crucible was closed.....  | 41 |
| 4.11 | XRD pattern of the diopside-based glass ceramic given by Öveçoğlu.....  | 42 |
| 4.12 | SEM micrographs of a glass ceramic sample containing 1 wt% of B <sub>2</sub> O <sub>3</sub> . The sample was heat treated at 650 °C for nucleation and at 850 °C for crystal growth when the lid of the crucible opened during melting..(a) X 2000 (b) X 10000..... | 46 |

|      |  |    |
|------|--|----|
| 4.13 | SEM micrographs of a glass ceramic sample containing 1 wt% of B <sub>2</sub> O <sub>3</sub> . The sample was heat treated at 650 °C for nucleation and at 1000 °C for crystal growth when the lid of the crucible opened during melting..(a) X 2000 (b) X 10000 .....  | 47 |
| 4.14 | SEM micrograph of the machinable glass ceramic given by Vogel et al.....   | 48 |
| 4.15 | SEM micrographs of a glass ceramic sample containing 2 wt% of B <sub>2</sub> O <sub>3</sub> . The sample was heat treated at 650 °C for nucleation and at 850 °C for crystal growth when the lid of the crucible opened during melting..(a) X 400 (b) X 12000 .....    | 49 |
| 4.17 | SEM micrograph of the sample star-like given by Shennawi....   | 50 |
| 4.16 | SEM micrographs of a glass ceramic sample containing 2 wt% of B <sub>2</sub> O <sub>3</sub> . The sample was heat treated at 650 °C for nucleation and at 1000 °C for crystal growth when the lid of the crucible opened during melting..(a) X 12000 (b) X 30000 ..... | 51 |
| 4.18 | SEM micrographs of a glass ceramic sample containing 4 wt% of B <sub>2</sub> O <sub>3</sub> . The sample was heat treated at 650 °C for nucleation and at 850 °C for crystal growth when the lid of the crucible opened during melting..(a) X 2000 (b) X 10000 .....   | 53 |

|      |   |    |
|------|---|----|
| 4.19 | SEM micrographs of a glass ceramic sample containing 4 wt% of B <sub>2</sub> O <sub>3</sub> . The sample was heat treated at 650 °C for nucleation and at 1000 °C for crystal growth when the lid of the crucible opened during melting..(a) X 2000 (b) X 10000 ..... | 54 |
| 4.20 | SEM micrographs of a glass ceramic sample containing 4 wt% of B <sub>2</sub> O <sub>3</sub> . The sample was heat treated at 650 °C for nucleation and at 1000 °C for crystal growth when the lid of the crucible opened closed melting..(a) X 2000 (b) X 10000 ..... | 55 |
| 4.21 | SEM micrographs of a glass ceramic sample containing 8 wt% of B <sub>2</sub> O <sub>3</sub> . The sample was heat treated at 650 °C for nucleation and at 850 °C for crystal growth when the lid of the crucible opened during melting..(a) X 2000 (b) X 10000 .....  | 57 |
| 4.22 | SEM micrographs of a glass ceramic sample containing 8 wt% of B <sub>2</sub> O <sub>3</sub> . The sample was heat treated at 650 °C for nucleation and at 1000 °C for crystal growth when the lid of the crucible opened during melting..(a) X 2000 (b) X 10000 ..... | 58 |
| 4.23 | SEM micrographs of a glass ceramic sample containing 8 wt% of B <sub>2</sub> O <sub>3</sub> . The sample was heat treated at 650 °C for nucleation and at 1000 °C for crystal growth when the lid of the crucible closed during melting..(a) X 500 (b) X 2000 .....   | 59 |

|      |   |    |
|------|---|----|
| 4.24 | SEM Micrograph of the samples given by Taira and Yamakj.....  | 62 |
| 4.25 | EDX analysis of the sample with 1 wt% of B <sub>2</sub> O <sub>3</sub> content was heat treated at 650 °C and 850 °C.....   | 64 |
| 4.26 | EDX analysis of the sample with 1 wt% of B <sub>2</sub> O <sub>3</sub> content was heat treated at 650 °C and 1000 °C.....  | 65 |
| 4.27 | EDX analysis of the sample with 4 wt% of B <sub>2</sub> O <sub>3</sub> content was heat treated at 650 °C and 850 °C.....   | 66 |
| 4.28 | EDX analysis of the sample with 4 wt% of B <sub>2</sub> O <sub>3</sub> content was heat treated at 650 °C and 1000 °C.....  | 67 |
| 4.29 | EDX analysis of the sample with 8 wt% of B <sub>2</sub> O <sub>3</sub> content was heat treated at 650 °C and 850 °C.....   | 68 |
| 4.30 | EDX analysis of the sample with 8 wt% of B <sub>2</sub> O <sub>3</sub> content was heat treated at 650 °C and 1000 °C.....  | 69 |
| 4.31 | EDX analysis of the sample with 4 wt% of B <sub>2</sub> O <sub>3</sub> content was heat treated at 650 °C and 1000 °C when the lid of the crucible was closed ..... | 70 |

4.32 EDX analysis of the sample with 8 wt% of B<sub>2</sub>O<sub>3</sub> content was heat treated at 650 °C and 1000 °C when the lid of the crucible was closed ..... 71

# CHAPTER 1

## INTRODUCTION

Glass ceramics are polycrystalline ceramic materials produced through controlled crystallization of glasses. Crystallization is accomplished by subjecting the suitable base glass to a regulated heat treatment involving the nucleation and growth of crystal phases in the glass[1].

Glass ceramics have a variety of unique thermal, mechanical, chemical, and dielectric properties[2]. Moreover, during manufacture complex shapes may be produced using standard glass forming techniques such as blowing, casting, drawing, and pressing prior to crystallization; and dimensional changes are small[1,3]. Dependent on their uniform reproducible fine grain microstructures, absence of porosity and wide ranging properties which can be tailored by changes in composition and heat treatment[3], they have found wide range of applications as engineering materials. Optical devices, transparent and opaque cooking ware, cooking top panels, heat resistant windows, telescope mirror blanks and biomedical applications are some of the examples where the glass ceramics are utilized[4]. A novel application of glass ceramics is military armour. New optical glass ceramics include integrated lens arrays, luminescent materials, and zero expansion passive optical materials, the latter recently used in the ring laser gyroscope[3]. Their new uses constantly appear.

Mica glass ceramics are new kind of glass ceramic composed of the  $\text{SiO}_2\text{-MgO-K}_2\text{O-F}$  system[5]. The predominant crystalline phase is synthetic fluormica,

named fluorophlogopite[6]. Minor additives such as CaO, Al<sub>2</sub>O<sub>3</sub> and TiO<sub>2</sub> may also be incorporated to modify or enhance the properties. In addition to unique thermal and chemical properties, mica containing glass ceramics provide machinability[7]. That is, they are cut, drilled, ground, turned, sawed, etc. Exceptional machinability results from interlocking plate like and easily cleavable mica crystals dispersed in a glassy matrix so that fine particles can be removed from the surface by pulverization[3].

Mica glass ceramics have generated interest in biomedical field, especially in the replacement of natural bone and dental restoration owing to their chemical inertness combined with high mechanical strength, appropriate thermal and biological properties[8]. The utilization of a machinable glass ceramic that can be melted and cast into the form of tooth has been marketed under different commercial names such as Dicor<sup>®</sup>, Macor<sup>®</sup>, Macerite<sup>®</sup>, and Bioverit<sup>®</sup>.

The microstructure of glass ceramics plays a great role in determining the properties and machinability[1]. Generally, the properties of mica glass ceramics are influenced by the amount and distribution of precipitated mica crystals along with the size and shape of grains[9] since they do not possess any porosity. The best machinability was secured where the product was highly crystalline and the crystals, themselves, were large and exhibited high aspect ratios. Products with such microstructure also provide high thermal shock resistance due to interlocking of the long platy crystals which allowed the products to adjust to thermal expansion and contraction[10]. M. J. Tzeng has reported that strength of mica glass ceramics can also be enhanced by obtaining well oriented microstructure and adding reinforcement elements like alumina and zirconia[8].

In spite of good peculiarities of mica glass ceramics, they have difficulties in their production. Mica glasses are very hard to prepare due to their high melting and forming temperatures (~1500 °C), large crystallization tendency, phase separation on cooling, compositional change due to volatilization of the fluorine, Mg and Si during melting[11,12]. A number of fluormica glass ceramics have

been found to swell and disintegrate when in contact with water[2]. Also, clinical failure of castable and machinable mica containing glass ceramics, because of insufficient mechanical performance, has been reported in the literature[5,7].

Mica glass ceramics can be considered as the latest technology in biomedical field. Although some commercial mica glass ceramic products have been utilized in dentistry, their detailed production processing route has not been given in the open literature. It has not been possible to find complete reference revealing the exact batch compositions and the factors affecting the processing conditions such as the heat treatment schedule that is necessary to precipitate phases from the glass. Efforts have been continuing to develop a new mica glass ceramic that will exhibit better performance. Recently, studies[13] have been conducted to overcome the difficulties in their production. Studies on the formation, microstructure and properties of mica glass ceramics have both technological and scientific significance. Therefore, it is necessary to execute a study directed towards the development of the most promising composition by investigating the microstructure and the properties.

Although some studies have been reported in the literature[1,6,10], for the effect of  $B_2O_3$  additions on the formation and microstructure of silicate systems, the information on the mica glass ceramics is yet limited and does not give a clear cut understanding. It would be scientific and technological interest to determine the role of  $B_2O_3$  additions on the formation and microstructure of the mica glass ceramics.

The present investigation was undertaken to accomplish two purposes. The first one was to determine the effects of small amounts of progressively increasing  $B_2O_3$  additions on the microstructure of mica glass ceramics. The second purpose was to develop a mica glass ceramic which would be produced at temperatures lower than 1500 °C.

## CHAPTER 2

### THEORY

#### 2.1. GENERAL

The discovery of fire and consequently the discovery that it would transform clay into ceramic pottery helped to improve the quality and length of the human life. Since then, ceramics have been used as materials for not only structural clay products such as pottery, porcelain, enamel, cement, refractories, abrasives, and glasses but also a variety of other products such as magnetic and optical materials, ferroelectrics, electronic ceramics, glass ceramics also others which were not in existence until a few years ago[14]. Within the last four decades another revolution has occurred in the ceramics to improve the quality of life. This revolution is the innovative use of specially designed ceramics for the repair and reconstruction of diseased or damaged parts of the body otherwise known as bioceramics[15].

Bioceramics involve the wide range of biomaterials; single crystals, polycrystallines, glasses, glass ceramics, and composites[16]. The utilization of all these bioceramics on the human body is shown in Figure 2.1. Conventional ceramics and glasses have been used for long time in the health care industry for eye glasses, dentistry, chemical ware, thermometers, and endoscopying. Soluble glasses have been used for carriers for enzymes, antibodies, and antigens[16]. Certain compositions of glasses, ceramics, glass ceramics and composites have been shown to bond to bone. These materials are called

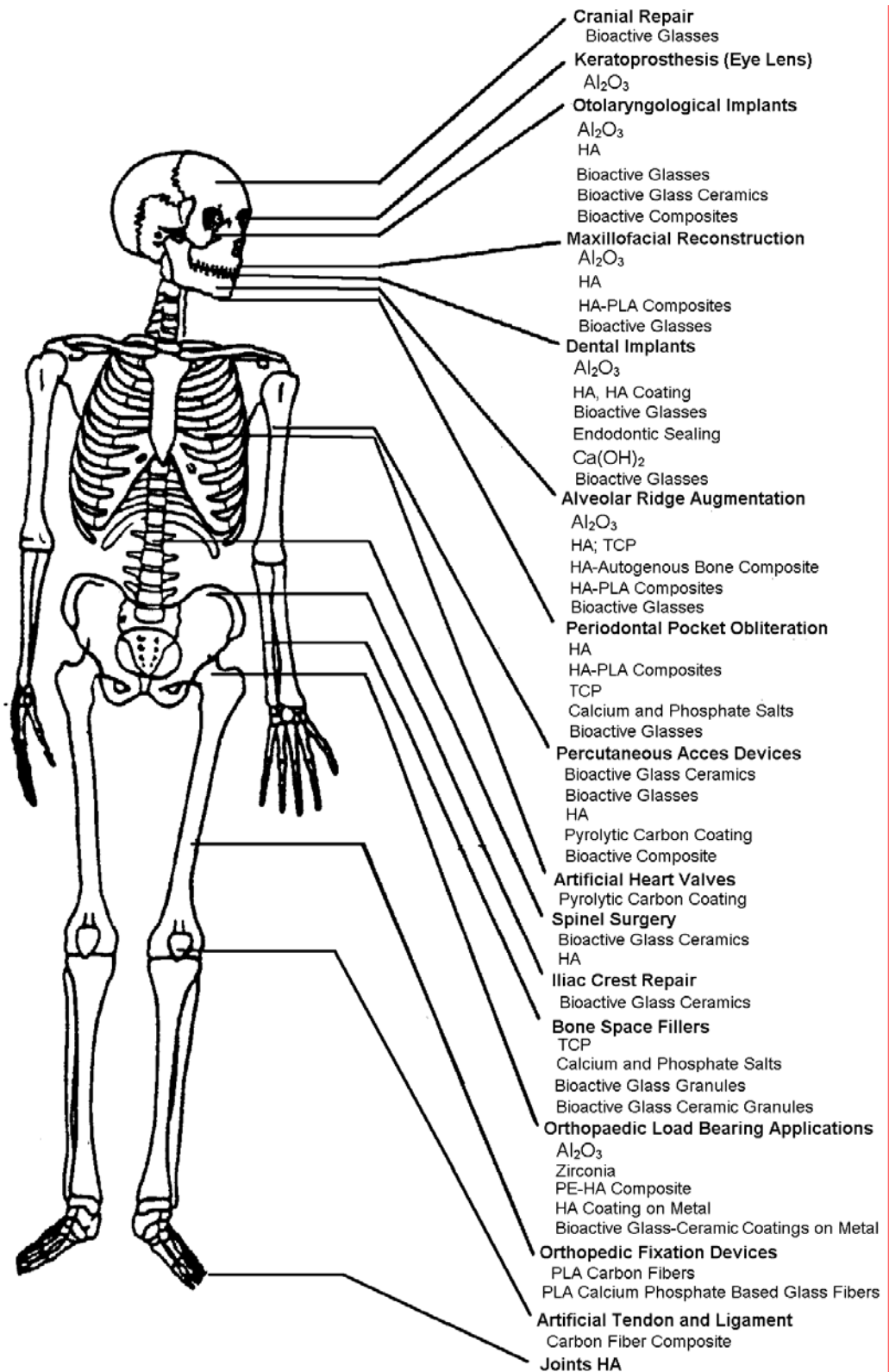


Figure 2.1. - Clinical uses of bioceramics[17]

bioactive ceramics. Some even more specialized compositions of bioactive glasses will bond to soft tissues as well as bone[18].

Many bioactive silicate glasses have been used for replacement of ear bones and maintenance of the jaw bone. The life of silica glasses for denture wears are 8 years, with nearly 80% retention rate[3]. Several other compositions that are bioactive, therefore, have been developed. Although many compositions have been tested, few have achieved human clinical application since clinical application success requires the simultaneous achievement of a stable interface with connective tissue and a match of the mechanical behaviour of the material with the tissue to be replaced[17]. It is known that for a bond with tissues to occur a layer of biologically active hydroxy calcium apatite (HCA) must form. The bond will not form if the rate of HCA formation is too low[19]. Consequently it has been concluded that bioactivity occurs only within certain ranges and very specific ratios of oxides in the  $\text{Na}_2\text{O-K}_2\text{O-CaO-MgO-P}_2\text{O}_5\text{-SiO}_2$  system[3]. However, the extents of these compositional limits are still not well understood.

The high uniformity of the microstructure of glass ceramics, the absence of porosity and the minor changes in volume during the conversion of glass into glass ceramic (usually only a few percent) make them attractive for many applications. Because the glass ceramic process begins with a glass, all the well established glass forming techniques can be employed to manufacture components with a variety of complex shapes including blowing, casting, rolling, pressing and rolling. Subsequently the glass component is converted into a fine grained polycrystalline solid by a heat treatment including nucleation and crystal growth[3].

A mica glass ceramic is a new kind of glass ceramic composed of the system  $\text{SiO}_2\text{-MgO-K}_2\text{O-F}$ . The predominant crystalline phase is synthetic fluormica, named phlogopite[6]. Minor additives such as  $\text{CaO}$ ,  $\text{Al}_2\text{O}_3$ ,  $\text{P}_2\text{O}_5$  and  $\text{TiO}_2$  may also be incorporated to modify or enhance the properties[7]. They exhibit not only good dielectric properties, excellent thermal shock resistance, good

mechanical strength and good corrosion resistance, but also very good machinability[6]. That is, they are cut, drilled, scratched and ground with normal metalworking tools. It has been shown that very high machinable precision in these materials can be achieved ( $\pm 10 \mu\text{m}$ ) using regular high speed tools[20]. Their machinability results in an increased versatility of the products and numerous possibilities of industrial application. The microstructural characteristic of these materials, consisting highly interlocked mica crystals embedded in a glass matrix, facilitate microfracture along the weak mica – glass interfaces and mica basal planes, avoiding macroscopic failure during machining[20]. The easy machinability of these materials results from the cleavage of interlocking layers of mica (phlogopite) crystals precipitated in the glass[9]. Phlogopite crystals are found in the form of flakes, needles and columns[21].

Generally, mechanical properties of glass ceramics are influenced by the particle size and amount and strength of the precipitated crystal since they do not possess any porosity. The bonding strength of interlayer ions is weakest in mica crystals, and the mechanical properties of mica crystals apparently are determined by the bonding strength of these interlayer ions[9]. The size of the mica platelets can be readily controlled through heat treatment, resulting in a significant effect on strength. The size of mica platelets also has a significant effect on the removal rate during machining with a dental diamond bur[22].

The heat treatment applied to the glass articles to cause the crystallization can be of vital importance in securing the desired extremely large flakes of fluormica. The preferred practice contemplates a schedule designed to produce very large fluormica crystals without sacrificing percent crystallinity. It is important to utilize high temperatures for the crystallization, i.e., the crystallization temperature should approach the deformation temperature of the body[10]. The cast ingot of glass should be heat treated, i.e, cerammed, to develop optimum physical and mechanical properties[8].

A castable and machinable mica containing glass ceramic, DICOR<sup>®</sup>/MGC (Dentisply, Milford, DE, USA) specifically designed for use in dental applications is recommended for the fabrication of crowns and veneers in aesthetic dentistry[5]. DICOR<sup>®</sup> is a glass ceramic of the SiO<sub>2</sub>-MgO-K<sub>2</sub>O-F system whose detailed composition in weight percent, wt%, is SiO<sub>2</sub>=56-64, MgO=15-20, K<sub>2</sub>O=12-18, F=4-9, and ZrO<sub>2</sub>=0.5-1. In order to obtain optimum strength and other desirable properties in the cast products, it is cerammed (heat treated) by subjecting to a special embedding procedure. The properties of DICOR<sup>®</sup> such as chemical durability, density, thermal conductivity, translucency, hardness, machining rates and wear rates are closely matched to those of human enamel[5].

## **2.2. GLASSES AND GLASS CERAMICS**

The first practicable glass ceramic materials were prepared nearly forty years ago. Since that time a wide variety of applications of these versatile materials have developed as a result of their many outstanding properties and distinct advantages of the glass ceramic method in certain circumstances over conventional ceramic processing routes. Of particular importance in many applications is the high uniformity of the microstructures of glass ceramics, the absence of porosity and the minor changes in volume during the conversion of glass into glass ceramic[23].

The manufacture of glass ceramic articles involves three steps. First, a glass forming batch is compounded to which a nucleating or crystallization agents are admixed; second, this batch is melted and the melt simultaneously cooled and shaped to get the desired shape and configuration of glass; and third, the glass article is heat treated with defined time and temperature schedule for having nucleation and growth of crystal phases in the glass[1]. Since the glass ceramic process begins with a glass, well established glass forming techniques can be employed to manufacture the components with a variety of complex shapes.

Subsequently, the glass component is readily converted into a fine grained polycrystalline ceramics by a controlled heat treatment.

The original glass ceramics were produced by inducing volume nucleation in melt derived bulk silicate glasses usually by the addition nucleating agents[3]. Recently, another method has been investigated instead of solid state reactions of each constituent compound or the recrystallization of solidified melts. In this method glass ceramics was prepared by the sol – gel process[24].

Glass ceramics are made by controlled crystallization, almost invariant contain a residual glass phase. Fundamentals of the controlled crystallization in glass has as its prerequisite a controlled phase separation. Phase separation is caused by the formation of stable molecular structural groups and their enrichment in a certain region[25]. In order to evaluate the properties of the glass ceramics, they must be considered to be multi-component materials with crystalline and glass phase. However, it is well known that the mechanical strength of glass and especially of invert glasses are very low[8].

The chemical stability and durability of glass ceramics are affected by the crystalline phase and also by the composition and the amount of the residual glass phase and its morphology[26]. The chemical composition of the residual glass phase is determined by the initial glass composition and the heat treatment. If the composition of the initial glass differs from that of the crystalline phase, then the composition and the volume fraction of the residual glass phase are continuously changing during heat treatment. This process can be stopped at any time by cooling the material and thus achieving the desired chemical composition of residual glass phase[13].

Glass ceramics are experienced because of their high strength and their machinability. A dense and homogenous glass ceramic containing apatite and wollastonite crystals is obtained when a glass powder compact in the system  $\text{MgO-CaO-SiO}_2\text{-P}_2\text{O}_5$  is heat treated on the appropriate heating schedule[23].

The glass ceramic shows an ability to form tight chemical bonds with living bone as well as high mechanical strength. This formation is investigated[27] by observing the microstructure; large cracks were formed in the crystallized product when the glass was heat treated in the bulk form. Formation of these cracks is attributed to the oriented precipitation of fibrous wollastonite crystals, on the grounds that no cracks were found in the glass which precipitated only apatite crystal. Oriented precipitation of crystals in a long fibrous form tend to induce a fairly large amount of directional volume change, causing large cracks in the interior of the crystallized product[28].

A glass ceramic is considered machinable if it can be turned, milled, drilled and tapped, with the same tools as used for machining metals, without breaking as normal ceramics would. Typically, the procedure is to cause in a certain base glass a controlled separation of mica crystals which have an optimum size for good machinability. The crystals should touch each other and account for about two thirds of the volume of the material. Machinability is provided by the fact that microfracture caused by machining preferably occurs along the preferred plane of the mica crystals. The phlogopite crystals make the material machinable. The machinability of the glass ceramic is somewhat reduced by the co-existing apatite crystals[29]. A controlled crystallization, two stage phase separation in glasses of the  $\text{Na}_2\text{O-K}_2\text{O-CaO-MgO-P}_2\text{O}_5\text{-SiO}_2\text{-Al}_2\text{O}_3\text{-F}$  system, followed by annealing results in both fluorophlogopite (mica) and apatite crystallization[29].

### **2.3. MICA STRUCTURE**

The micas are layered silicates with the foliform habit and show excellent cleavage at the (001) plane. The alkali ions are sandwiched between the three layer packets which results in very weak connections. The (001) plane of the mica crystals are preferred as a direction of cleavage when the glass ceramic are machined. Due to a great number of interlocking mica crystals in the glass ceramics, the microfractures caused by mechanical processing easily propagate

from crystal to crystal, resulting in removal of material without breaking the part[30].

The micas involve two units; one consisting of closely packed oxygen and hydroxyl or fluorine in which cations of radii 0.05 to 0.08 nm are present in octahedral coordination[23]. The other unit is built of silicon – oxygen tetrahedra linked together in a hexagonal network so as to form a sheet of a Si:O ratio of 4:10. The basic structure is therefore a composite sheet in which a layer of octahedrally coordinated cations is sandwiched between identical layers of tetrahedral sheets pointing toward each other. The three layer composite sheet has a net negative charge arising from substitutions. The excess charge is balanced by uptake of large cations between the composite sheets in 12- fold coordination. The interlayer cations are weakly bonded, giving rise to a perfect set of basal cleavage. Their structure is characterized by the loose connection via  $K^+$  or  $Na^+$  ions layer packets as seen in Figure 2.2. These layered packets in turn consist of two tightly connected  $(Si_2O_5)^{2-}$  layers. Characteristically, each fourth tetrahedron (a cross section vertical to the plane in Figure 2.2) in such a layer of six rings of tetrahedra is an  $AlO_4$  tetrahedron. The firm connection of a layer packet is achieved by  $Mg^{2+}$  and  $F^-$  ions in the form of brucite layer. In special cases, where these have a strong tendency to hydrate, water swelling and consequent lattice expansion result.

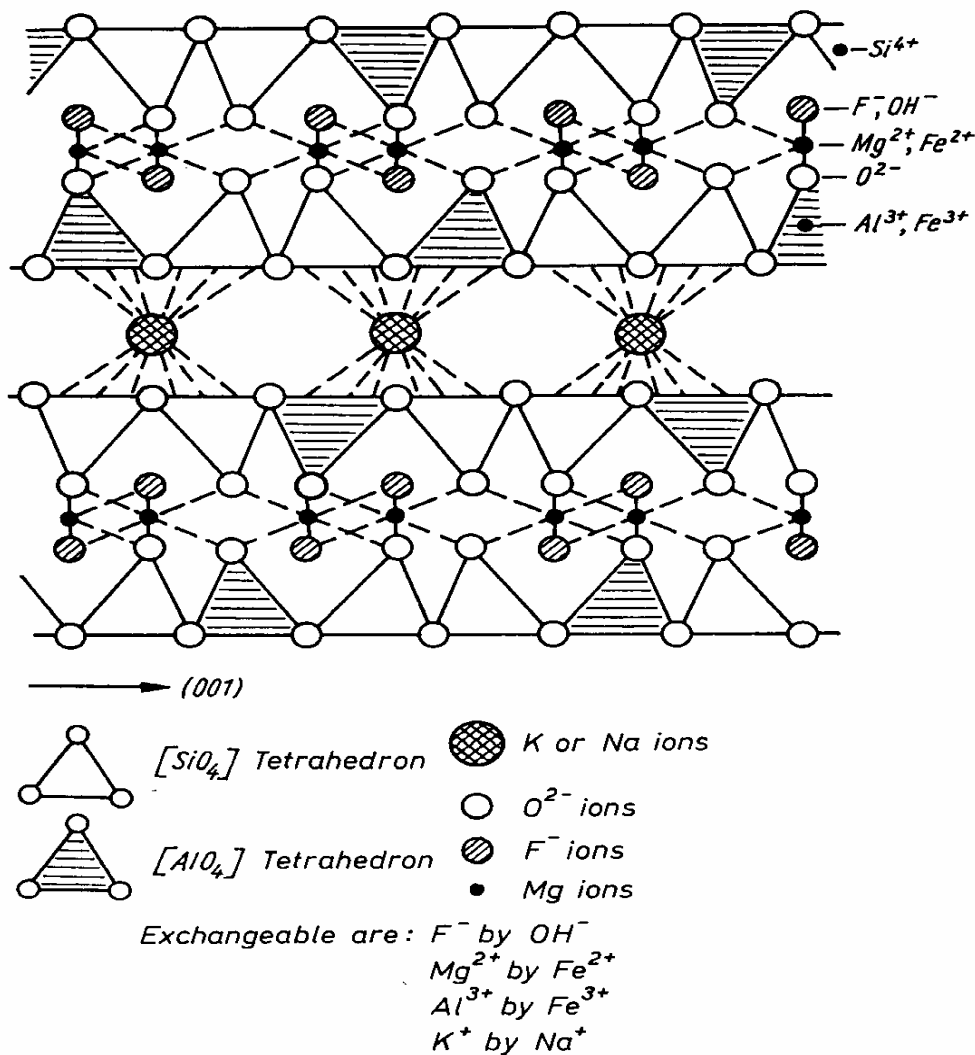


Figure 2.2 - Schematic of Fluorophlogopite Structure[23]

The  $\text{Mg}^{2+}$  ions are bonded directly to  $\text{O}^{2-}$  ion, which represent corners of tetrahedra. The second valence of the  $\text{Mg}^{2+}$  ion is satisfied by the  $\text{F}^-$  ion, which is always located in the center of six ring tetrahedra. In this way, the tetrahedron layers appear interlocked. The  $\text{Mg}^{2+}$  ion may be replaced by an  $\text{Fe}^{2+}$  ion, the  $\text{F}^-$  ion by an  $\text{OH}^-$  ion. Also all  $\text{Mg}^{2+}$  ions connecting the two tetrahedron layers are in six coordination as shown in Figure 2.2. Such three layer packets are loosely connected  $\text{K}^+$  and  $\text{Na}^+$  ions. These alkali ions function as a charge balance for the unsatisfied oxygen valences of protruding  $\text{SiO}_4$  and  $\text{AlO}_4$  tetrahedra. The bonding strength of interlayer ions is weakest in mica crystals, and the

mechanical properties of mica crystals apparently are determined by the bonding strength of these interlayer ions[9].

The chemical formula of mica is expressed as  $X_{0.5-1}Y_{2-3}Z_4O_{10}(OH,F)_2$  where X, Y, and Z are cations in 12-, 6-, and 4- fold coordination, respectively. Extensive solid solutions occur due to the substitutions or unoccupied sites. Highly crystalline glass ceramics are obtainable from clear glasses in the RO-Al<sub>2</sub>O<sub>3</sub>-SiO<sub>2</sub>-F system, where RO represents alkaline earth oxides. The nucleation crystallization involves; microphase separation → internal nucleation of MgF<sub>2</sub> → crystallization of trisilicic alkaline earth mica crystals on MgF<sub>2</sub> nuclei[31]. The crystallization sequence for tetrasilicic fluorophlogopite mica (R<sub>0.5</sub>Mg<sub>3</sub>AlSi<sub>3</sub>O<sub>10</sub>F<sub>2</sub>, where R= K, Ca, Sr, Ba) consists of several steps, and these steps for alkaline earth mica glass ceramics are quite different from their alkali counterparts. Yet MgF<sub>2</sub> has been found to play a role in the crystallization process in both of these systems[5].

If the aggregate content of (Al<sub>2</sub>O<sub>3</sub>+MgO) in the glass is increased at the cost of SiO<sub>2</sub>, part of the Mg ions in the new mica crystals are replaced by Al ions. As a result, the octahedron layer of the mica fabric develops stresses which cause the crystal to bend. An added effect of that state is a change of the dioctahedron trioctahedron character of the crystals. If the (Al<sub>2</sub>O<sub>3</sub>+MgO) concentrations in the base glass were increased still further, rings of tetrahedrons would be formed, thus producing cordierite crystals. The AlO<sub>4</sub> in cordierite crystals are stabilized by Mg<sup>2+</sup> ions. The machinability of glass ceramic having fluorophlogopite crystals of the new shape is four to five times better than that of the materials with flat mica flakes[32,33].

Another very important influence on the machinability is crystal size. It has been observed that[23] glass ceramic with very small fluorophlogopite crystals can be machined but not as well as the one with large crystals. This might be understood in terms of repeated energy requirements for new cleaving processes if the fracture spread fails too quickly. It has been established that there is optimal crystal size.

## 2.4. CRYSTALLIZATION OF GLASSES

The nucleation and crystallization of glass are important processes which need to be known in order to form glass ceramics with the desired structure and properties. The crystallization sequence and many other details as determined by Scanning Electron Microscopy (SEM) and X – ray diffraction (XRD) of glass ceramics, which include alkali metal containing and alkaline earth containing, are available[5]. The investigation of the crystallization of glasses is of importance both scientifically and technologically. Glass formation itself implies the avoidance of crystallization during the cooling of a melt. On the other hand, the production of glass ceramics requires the achievement of controlled crystallization leading to the formation of the desirable fine grained microstructure while avoiding crystallization during cooling and shaping of the material[26].

The application of controlled crystallization in the production of glass ceramics requires that attention to be paid to both nucleating and growth rates. If the former rate is too low, growth will take place from too few centers and a coarse grained microstructure is likely to result. Also if the crystal growth rate is too high, coarsening of the microstructure can result[26].

Differential thermal analysis (DTA) is used extensively to understand the crystallization kinetics of glasses[34-38]. It should be noted that the appearance of an endothermic asymmetric minimum peak and an exothermic asymmetric maximum peak in the DTA curves during the non-isothermal heating corresponds to the nucleation and crystal growth, respectively. If an exothermic peak follows an endothermic peak, it would be indicative that the growth followed after the nucleation has been completed. Further, if the transformation processes take place simultaneously, the thermal effect of nucleation and the thermal effect of growth will overlap, and the asymmetric feature of the curve will be less pronounced[39].

Crystal nucleation may be either homogeneous or heterogeneous but in glasses it is found that homogeneous nucleation is comparatively rare except for some glasses of simple composition. In most cases, heterogeneities must be present since these can lower the activation energy of nucleation if wetting of heterogeneity by the precipitated phase occurs[26].

It is an established fact that almost every crystallization in glass has a controlled phase separation. Phase separation is caused by the formation of stable molecular structural groups and their enrichment in certain regions. The production of glass ceramics requires the generation of a high of nucleating sites within the bulk of the material. For this purpose, a nucleating agent is incorporated into parent glass compositions. The most important group of nucleating agents comprises certain oxides including  $\text{TiO}_2$ ,  $\text{P}_2\text{O}_5$ ,  $\text{ZrO}_2$ [26].

A realistic basis for the production of glass ceramics prescribes a heat treating schedule as shown in Figure 2.3. Forming and annealing of molten clear glass occur during step 1 (Glass processing). Step 2 (Nucleation) which leads to nucleation, involves subsequent reheating the glass to temperature  $T_1$  (nucleation temperature) and holding at this temperature for defined time periods. In step 3 (Crystallization), a further temperature increase to  $T_2$  (growth temperature), and holding at this temperature for defined time periods take place. Crystallization is completed after the third step. Step 4 (Cooling) represents the cooling of the final product to ambient temperatures[13].

The first holding temperature in step 2 represents the further development of phase separation, where nucleation of the crystals may, but need not, occur. But all the prerequisites for the nucleation obtained in this step. During the second holding in step 3, the glass changed to the glass ceramic product[23].

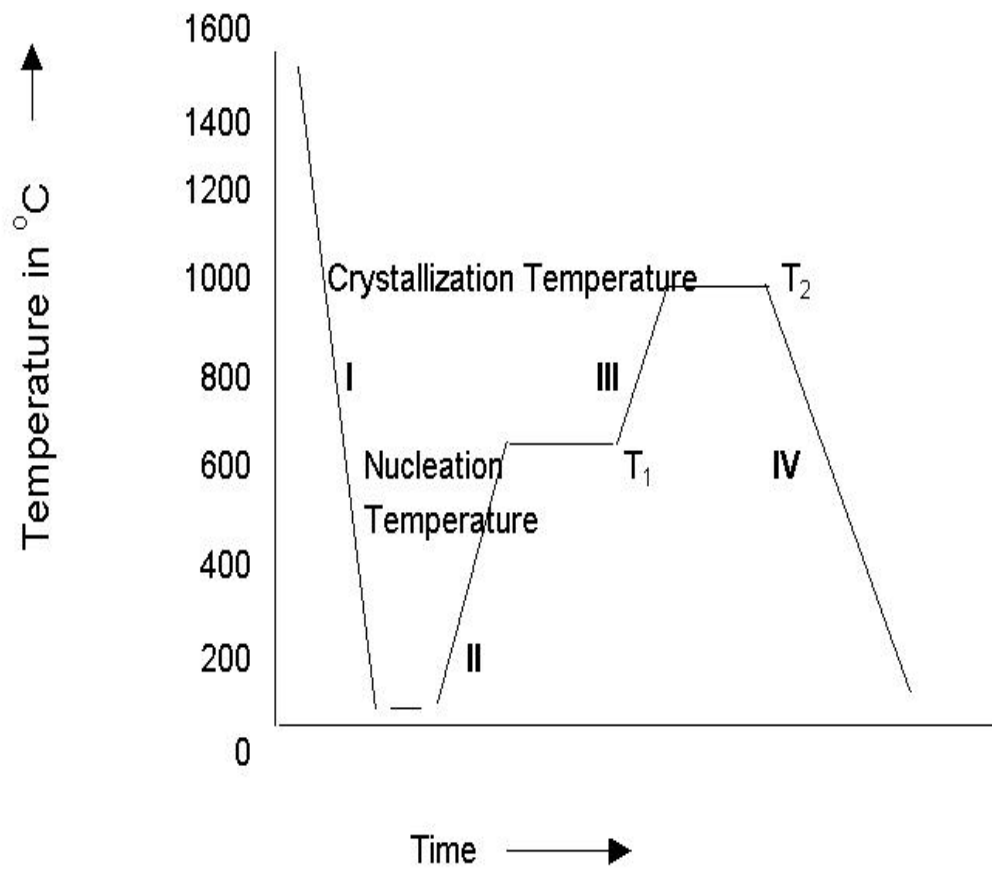


Figure 2.3 Schematic of the formation of a glass ceramic.

- I – Glass processing
- II – Nucleation
- III – Crystallization
- IV – Cooling

## 2.5. EFFECT OF TiO<sub>2</sub> ON GLASS – CERAMICS

Titanium dioxide, TiO<sub>2</sub>, is commonly used as nucleating agent. Addition amount generally does not exceed 2 weight percent, wt%, of glass. TiO<sub>2</sub> additions can have remarkable influence on the crystallization behavior of glasses in the MgO-Al<sub>2</sub>O<sub>3</sub>-SiO<sub>2</sub> system[11].

Liquid phase separation occurs first in glass ceramics with TiO<sub>2</sub> added as a nucleating agent, then crystalline compounds or solid solution containing TiO<sub>2</sub> and some components of the glass (MgO.TiO<sub>2</sub>) or TiO<sub>2</sub> itself precipitate as a high density of fine crystals. Consequently, these crystals act as nuclei for crystallization of main crystalline phase. TiO<sub>2</sub> may also act as a surface active agent and increase the nucleation rate[40]. Addition of Al<sub>2</sub>O<sub>3</sub> in combination with TiO<sub>2</sub> and SiO<sub>2</sub> promoted fine – scale volume crystal nucleation[3].

The incorporation of a small amount of TiO<sub>2</sub> decreases the glass transition temperature significantly, and further decrease of T<sub>g</sub> is observed as TiO<sub>2</sub> content increases. This is attributed to a reduced number of bridging bonds in the silica based network leading to a decrease of the viscosity and, consequently, of the glass transition temperature[41].

The addition of TiO<sub>2</sub> always reduces the liquidus temperature, T<sub>L</sub>, owing to the formation of eutectics with SiO<sub>2</sub>[40]. Also, the addition of TiO<sub>2</sub> improves both of the nucleation and growth rates of apatite by decreasing the viscosity and decreasing the surface energy between crystal and glass[40]. TiO<sub>2</sub> additions enhance the formation of phlogopite, also. For two step heat treatment, the TiO<sub>2</sub> content should not exceed 2%, beyond this point it causes disadvantage situation for formation. When the TiO<sub>2</sub> content is increased to 2%, fluorophlogopite formation is reduced and some TiO<sub>2</sub> crystals begin to form[42].

## 2.6. EFFECT OF MgF<sub>2</sub> ON GLASS – CERAMICS

Magnesium fluoride, MgF<sub>2</sub>, is used as the source of the fluorine in glass ceramics. The amount of F was varied while holding the Mg content constant by adjusting the amount of MgO. If MgF<sub>2</sub> is compared with NaF as the fluorine source, MgF<sub>2</sub> has some advantages. 28-34% and 8-15% fluorine was lost in the prepared NaF and MgF<sub>2</sub> glasses, respectively[43]. The loss of fluorine is primarily due to volatilization of fluorine from the glass melts. Increasing melting temperature, melting time, or use of an uncovered crucible would significantly increase the fluorine loss in glasses. The loss of volatile components was also observed when melting other glass compositions. For the glass batches containing the same amount of fluorine, the fluorine loss is 1-2 times higher when NaF was used as the fluorine source than when MgF<sub>2</sub> was used[43].

The glass with the fluorine source of MgF<sub>2</sub> shows uniform bulk crystallization and forms mica containing glass ceramics after heat treatment[44]. Besides the Si-O-Si network in silicate glasses, Raman spectrum shows that boroxol rings are main boron units in the NaF borate glasses, while other three- or four-coordinated boron units, such as chain type metaborate groups, pentaborate groups, diborate groups, highly changed orthoborate groups and pyroborate groups, are present in MgF<sub>2</sub> borate glasses[44].

## 2.7. EFFECT OF B<sub>2</sub>O<sub>3</sub> ON GLASS – CERAMICS

Mica glass ceramic articles containing fluorophlogopite as the predominant crystal phase can be produced from the system consisting of essentially, Na<sub>2</sub>O-K<sub>2</sub>O-CaO-MgO-Al<sub>2</sub>O<sub>3</sub>- B<sub>2</sub>O<sub>3</sub>-SiO<sub>2</sub>-F.

Besides SiO<sub>2</sub>, B<sub>2</sub>O<sub>3</sub> is also a glass former oxide. The stability of the boron containing glasses is also dependent on the chemical states of boron ions in the

glasses[44]. Laboratory experience in literature has demonstrated that at least 10 wt% MgO is required; where B<sub>2</sub>O<sub>3</sub> is present alone at least the minimum amount of B<sub>2</sub>O<sub>3</sub> permits the attainment of the fluorophlogopite crystallization with less than 10 wt% MgO[10].

It is not known whether B<sub>2</sub>O<sub>3</sub> enters into the fluorohlogopite structure but its presence is useful in reducing the surface tension of the melt, thereby assisting rapid crystallization growth, and in stabilizing the residual glass[45]. J.E. Flannery has reported[45] that the molten batch appeared to stiffen in the manner of a normal glass melt until a temperature of about 875-1050 °C was reached. At or about that temperature range, a hazy opalization took place at the edges of the slab and moved toward the center thereof. A wave of opaque crystallization followed closely behind. The inclusion of B<sub>2</sub>O<sub>3</sub> is helpful in obtaining very rapid crystallization. It also appears to alleviate warping tendencies which have been observed as a result of the rapid crystallization.

The outward appearance of the crystallized products is quite similar to that of conventional glass ceramic articles, being opaque and white. The surface quality, especially those compositions containing B<sub>2</sub>O<sub>3</sub>, demonstrated satiny finish. In general, the crystalline bodies are quite strong with modulus of rupture values varying between about 103.5-241.5 MPa on unbrained samples[45]. The coefficients of thermal expansion (room temperature to 300 °C) commonly range between about 60-90 x 10<sup>-7</sup> / °C.

The microstructure of the glass – ceramic article is of vital significance in determining the mechanical and electrical properties thereof. In compositions containing less than about 5% B<sub>2</sub>O<sub>3</sub>, the percentage of crystallinity can be as high as about 65 % by volume but aspect ratio of the crystals is not great, averaging about 3-4:1[1]. This result is in a product exhibiting some machineability but with good mechanical strength, sometimes demonstrating a modulus of rupture in excess of 138 MPa. There is only limited interlocking of the mica crystals and, as would be expected, the dielectric properties,

mechanical strength properties, and thermal shock resistance do not closely approach those of sheet mica.

In the microstructure of the fluorophlogopite obtained utilizing  $B_2O_3$  contents greater than 5% by weight, large interlocking platelets of mica with high aspect ratio were readily apparent. The texture resembles a house of cards. This house of cards microstructure has manifested the best properties with respect to mechanical and thermal shock resistance and has provided dielectric properties approaching those of naturally occurring sheet phlogopite[1]. With the glass composition containing less than 5% by weight  $B_2O_3$ , magnesium fluoride (sellaite) is the first phase to crystallize and can be readily identified through XRD analysis. With the glass composition containing more than 5% by weight  $B_2O_3$ ,  $MgF_2$  is normally not the first crystal phase to precipitate. Instead, fluoroborite, is formed which is also readily identifiable through XRD analysis. Like  $MgF_2$ , fluoroborite is stoichiometric with a composition  $Mg_3BO_3F_3$ [1].

Shi and James[46-48] have shown that addition of  $B_2O_3$  also promotes volume nucleation in glass ceramics. The crystallization mechanism and nucleation kinetics in the 20 mol%  $B_2O_3$  glass were studied using XRD, electron microscopy and quantitative optical microscopy. Volume crystal nucleation occurred after heat treatments near the glass transformation temperature  $T_g$  (613 °C). The first phase to precipitate was  $BPO_4$  and subsequently the phase  $4CaO.P_2O_5$  appeared by heterogeneous nucleation on the  $BPO_4$ .

$B_2O_3$  in glass ceramics increases the viscosity at low temperature however decreases the viscosity at high temperature, raises the crystallization temperature, allowing densification prior to crystallization[49]. The addition of the  $B_2O_3$  tends to further promote grain growth of the fluormica flakes by indicating the fluidity of the growth medium[10].

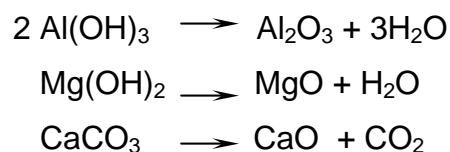
## CHAPTER 3

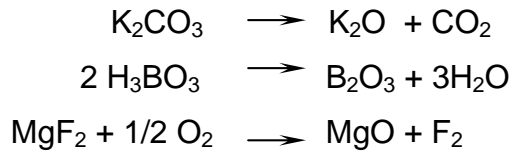
### EXPERIMENTAL PROCEDURE

#### 3.1 SAMPLE PREPARATION

##### 3.1.1 Batch materials

The characteristics of the initial materials have great influence on the formation and the structure of the glass ceramic material produced as they affect the reproducibility. Purity and toxicity are important characteristics since the final product is to be used in the human body. The raw materials must not include any toxic material since they are harmful for human health. Moreover, toxic materials decrease the biocompatibility of implant materials[13]. Therefore, extra pure grade chemicals in powder form were used as starting materials in this study. The powders were supplied from Merck Co., Germany. The sources of silica and titania were  $\text{SiO}_2$  and  $\text{TiO}_2$ . Fluorine was added into composition as  $\text{MgF}_2$ . The raw materials for  $\text{CaO}$  and  $\text{K}_2\text{O}$  were their carbonates;  $\text{CaCO}_3$  and  $\text{K}_2\text{CO}_3$ , respectively.  $\text{Al}(\text{OH})_3$  and  $\text{Mg}(\text{OH})_2$  were used to obtain  $\text{Al}_2\text{O}_3$  and  $\text{MgO}$ , respectively.  $\text{H}_3\text{BO}_3$  was used for the source of  $\text{B}_2\text{O}_3$ . The raw materials were assumed to decompose into their stable oxides during melting as follows:





### 3.1.2 Formation of Glasses

On the basis of the formation of a mica glass ceramic a batch composition given in Table 3.1 was taken under consideration. Der[13] has reported that a glass is formed from this composition from which a mica based glass ceramic for dental applications can be produced upon subjecting a suitable heat treatment. The change in batch composition was done only by introducing  $\text{TiO}_2$  and  $\text{H}_3\text{BO}_3$  to batch.  $\text{TiO}_2$  was added into all batches as a nucleating agent in the amounts of 1 weight percent (wt%) of the glass.  $\text{H}_3\text{BO}_3$  additions were made accordingly to obtain 1, 2, 4, and 8 wt%  $\text{B}_2\text{O}_3$  in the final glass composition. The ingredients, batch and final compositions of the glass investigated were tabulated in Table 3.1.

The raw materials were carefully weighed ( $\pm 0.0005$  g) to their proper amount in an electronic balance and mixed in an agate mortar with pestle to prepare batches. Isopropyl alcohol was used in mixing medium. The total weight of each batch was 15 grams. Besides batch ingredients,  $\text{H}_3\text{BO}_3$  and  $\text{TiO}_2$  were added into batch in the amounts when necessary. Then, the mixtures were placed into an oven to get rid of alcohol at about  $80^\circ\text{C}$  for approximately 12 hours. This procedure was applied to all batches prior to melting.

The batches were placed in a platinum crucible and melted in it at  $1400^\circ\text{C}$  in electrically heated muffle furnace. The melt was kept at this temperature for 20 minutes to ensure the homogeneity of the melt. Melting took place in normal laboratory conditions without controlling the atmosphere. When melting was complete, the crucible and its content were taken immediately out of the furnace and dipped into cold water without contacting glass to water.

Table 3.1 The ingredients, batch and final compositions of the glass investigated

| Ingredients                    | Batch Composition (wt %) | Final Composition* (wt %)                |
|--------------------------------|--------------------------|--|
| SiO <sub>2</sub>               | 50.73                    | 56.70 as SiO <sub>2</sub>                |
| K <sub>2</sub> CO <sub>3</sub> | 23.21                    | 17.67 as K <sub>2</sub> O                |
| Al(OH) <sub>3</sub>            | 0.8                      | 0.59 as Al <sub>2</sub> O <sub>3</sub>   |
| Mg(OH) <sub>2</sub>            | 10.42                    | 15.02 as MgO                             |
| MgF <sub>2</sub>               | 8.98                     | 6.20 as F                                |
| CaCO <sub>3</sub>              | 5.86                     | 3.82 as CaO                              |
| TiO <sub>2</sub>               | -----                    | 1 as TiO <sub>2</sub>                    |
| H <sub>3</sub> BO <sub>3</sub> | -----                    | 1-2-4-8 as B <sub>2</sub> O <sub>3</sub> |

\*Calculated assuming the batch ingredients were decomposed into their stable oxides.

### 3.1.3 Preparation of Glass – Ceramics

Glass pieces were converted to glass ceramics through the controlled crystallization. Controlled crystallization was performed by a double step heat treatment including nucleation and growth of crystal phases. That is, the glass samples were heated first to the nucleation temperature, the temperature at which the nuclei formed, and then to growth temperature, the temperature where nuclei growth occurred. The nucleation temperature was taken as 650 °C. Two different growth temperatures (850 °C and 1000 °C) were applied to determine the crystalline phases and microstructure formed after each temperature. The samples were held at the nucleation and crystal growth temperatures for defined time periods. The time duration at which the samples were held at the nucleation temperature (hereafter will be called as nucleation time) and the time duration at which the samples were held at the crystal growth

temperature (hereafter will be called as growth time) were kept constant at 8 hours.

A heating rate of 3 °C/min was kept constant for both nucleation and crystal growth periods. After holding the samples at the growth temperature for defined time, furnace was cooled at the same rate to room temperature. Heat treatment schedule used in this study is shown schematically in Figure 3.1.

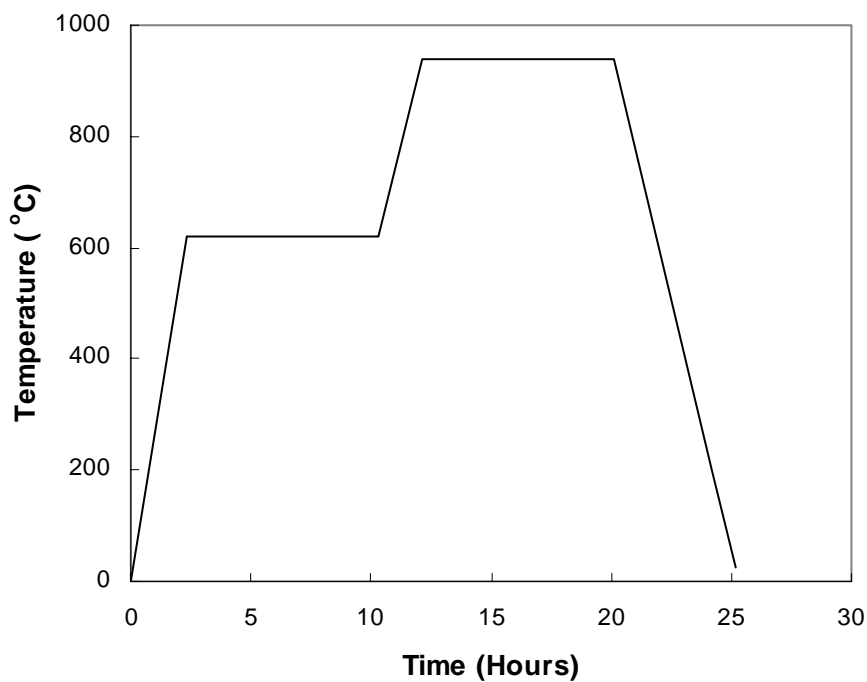


Figure 3.1 Schematic representation of the heat treatment applied to convert the glass to glass ceramic.

After the heat treatment, the samples appeared in white (milky) color. The appearance of the samples indicated that phase separation occurred during cooling of the glass. It was obvious from the appearance of the samples that at least two phases crystallized during heat treatment.

## **3.2 ANALYSES**

### **3.2.1 X – Ray Diffraction (XRD)**

Powder XRD analyses were performed on glass samples and the corresponding crystallized counterparts for each composition (i.e samples containing no, 1, 2, 4 and 8 wt% B<sub>2</sub>O<sub>3</sub>) to identify the crystal phases precipitated due to the course of crystallization. The XRD patterns were obtained using a Rigaku type diffractometer (Ultima SA-HFJ) with Ni-filtered CuK<sub>α</sub> radiation. Each sample was scanned from 5 to 85 degrees 2θ at 2 degrees per minute by 0.05 degrees continuously.

### **3.2.2. Differential Thermal Analysis (DTA)**

Glass samples of four different compositions, having 1, 2 , 4 and 8 wt % of B<sub>2</sub>O<sub>3</sub> were ground into powders of approximately 45-75μm and were examined using a DTA unit was NETZSCH Geratebau GmbH Sleb Bessell. The powdered sample was heated in a Pt-holder against another Pt-holder containing α- Al<sub>2</sub>O<sub>3</sub> as a standard material. A uniform heating rate of 10 °C/min was adopted up to the appropriate temperature of the glasses. The results obtained were used as a guide for determining the heat-treatment temperatures applied to induce crystallization.

### **3.2.3 Scanning Electron Microscope (SEM)**

The crystallization characteristics and internal microstructures of the resultant materials were examined by using SEM, where representative electron micrographs were obtained using Jeol, JSM–6400, scanning electron microscope. A thin layer of Au-Pd alloy was coated onto samples prior to SEM

studies. Also, Energy Dispersive X-ray (EDX) analysis was performed for some specimens to determine the chemical compositions.

Schematic representation of the experimental procedure carried out in this study is shown in Figure 3.2.

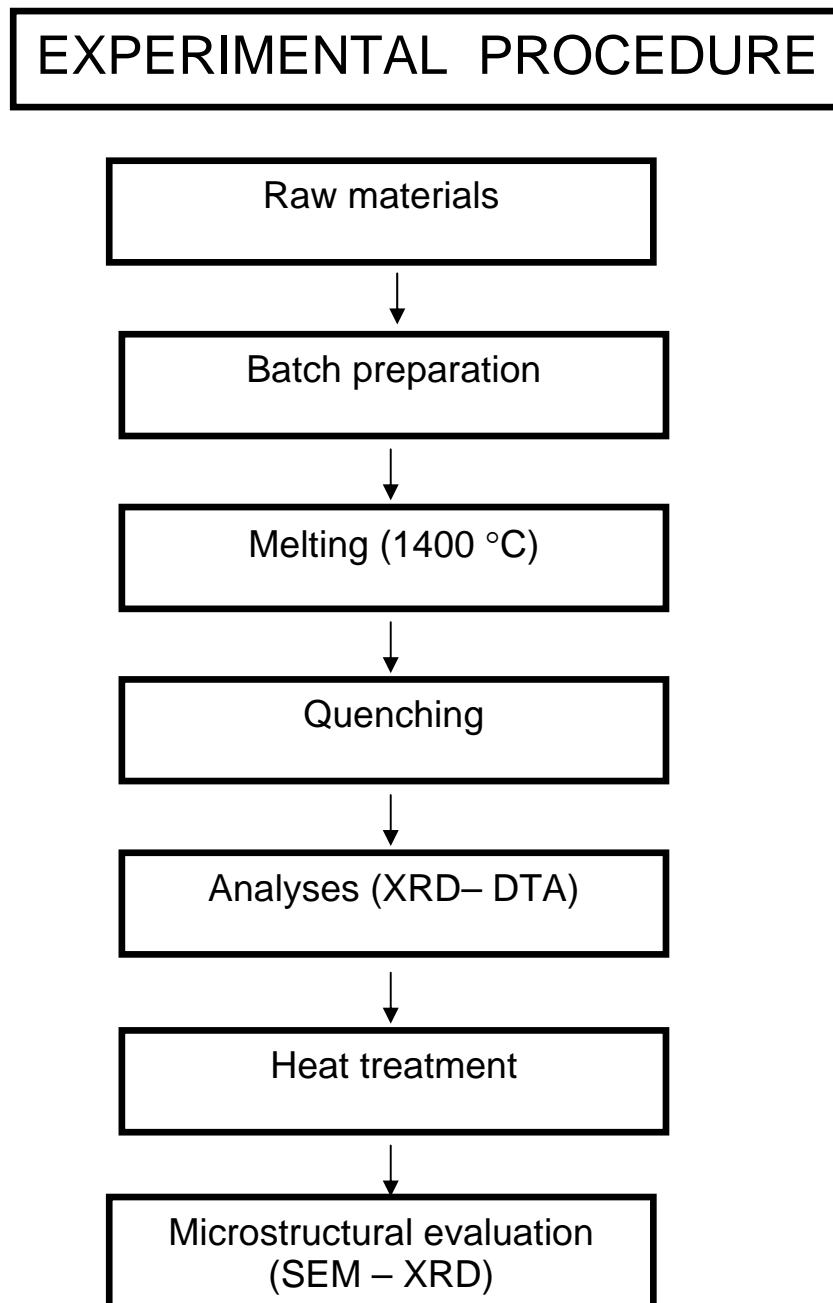


Figure. 3.2 Flow chart of the experimental procedure.

## CHAPTER 4

### RESULTS AND DISCUSSION

#### 4.1 GENERAL

Data obtained during experimental studies of the thesis work were presented and discussed in this chapter.

Glasses containing no, 1, 2, 4, and 8 wt%  $B_2O_3$  were formed according to the procedure as described in Section 3.1.2. The as-formed glasses of different compositions were converted to glass ceramics as described in Section 3.1.3. Thermal, structural, and phase analyses were performed as described in Section 3.2 to understand the effects of small amounts of progressively increasing  $B_2O_3$  additions on the microstructure of mica based glass ceramics. Data were gathered through direct observations and quantitative measurements obtained during the analyses.

##### 4.1.1 Formation of Glasses

The melting temperature of mica based glasses was commonly accounted around 1500 °C. One of the objectives of this study was to develop a mica glass ceramic which will be produced at temperatures lower than 1500 °C. In order to accomplish this objective the batch materials were melted at 1400 °C as described in Section 3.1.2 to see the effect of  $B_2O_3$  on the melting temperature.

Batches yielded clear and transparent glasses upon melting at 1400 °C. Glasses were obtained easily for each of the compositions studied. Physical appearance of the glass pieces has suggested that the product was totally glass. That is, they did not indicate any evidence of unmolten batch materials or crystallinity. In order to assure the glassiness of the samples powder X-Ray Diffraction (XRD) analyses were performed as described in Section 3.2.1. Representative XRD patterns of the as-formed glasses containing 1 wt% B<sub>2</sub>O<sub>3</sub> and 4 wt% B<sub>2</sub>O<sub>3</sub>, shown in Figure 4.1, did not illustrate any crystal peaks resulting from the reflection of intensity beam from definite crystallographic planes in crystal. The patterns illustrated a hump at low 2θ values which is an indicator of short range order, i.e. glass.

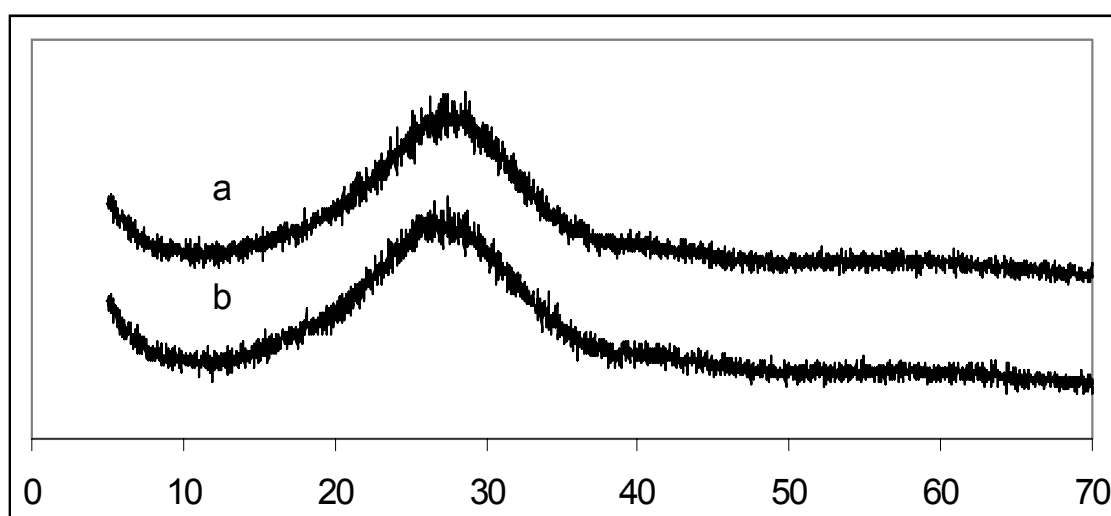


Figure 4.1 a) The XRD pattern of the glass containing 1 wt% B<sub>2</sub>O<sub>3</sub>  
b) The XRD pattern of the glass containing 4 wt% B<sub>2</sub>O<sub>3</sub>

It has been reported that[11,12] compositional changes due to volatilization of fluorine may occur during melting of this kind of glasses. Crucible top was covered with a lid during melting since there is a possibility of fluorine volatilization during glass melting. It has been also suggested that[11,12] covering of the crucible top with a lid during melting may be effective in terms of minimizing or eliminating the fluorine volatilization occurring through the glass making procedure so that the fluorine content in glass composition remains unchanged. However a recent study conducted by Der[13] has revealed that covering of the crucible top with a lid during melting did not have much influence on the volatilization of fluorine. He has melted glasses of the same composition while the crucible was or was not covered with a lid during melting and performed wet chemical analyses on the as-formed glasses. He concluded that even though there is a slight difference between analyzed compositions of the two glasses, both analyses results matched up with each other. Therefore, fluorine volatilization occurred throughout the glass making procedure in this work was ignored. At the meantime, some of the batches were melted while the crucible was covered with a lid during melting to see if there is a difference between these two cases in terms of the phases developed and microstructure in this material.

To get the maximum homogeneity of the melt without vaporization of the fluorine, the melt was held at the peak temperature for approximately 20 minutes. There is no consensus among the scientists about the holding time of the melt at the peak temperature. However, it is usually taken as a few minutes and generally varies with the amount of batch[45,50-52]. It has been also reported that[1,10] the total time spent for heating the batch materials to the melting temperature and holding the melt at this temperature was about 5-6 hours. However, this long time periods might cause an increase in the fluorine evaporation. Therefore, the total time period for melting the batch materials in this study was approximately 2.5 hours.

After completion of the melting procedure, the melt was tried to cast onto stainless steel plates but due to the insufficient fluidity for casting, it was allowed to solidify in the crucible. Solidification was accomplished by dipping the crucible and its contents into cold water without contacting melt with water.

#### 4.1.2 Preparation of Glass Ceramics

A piece of as-formed glass from each composition were subjected to a controlled heat treatment as described in Section 3.1.3 in order to convert the glass pieces to glass ceramics. The double step heat treatment was applied to all glasses. The nucleation and growth temperatures were determined from a Differential Thermal Analysis (DTA). A representative DTA thermogram for the as-formed glass containing 1 wt% B<sub>2</sub>O<sub>3</sub> shown in Figure 4.2 indicated three distinctive features: the slight endothermic minima at approximately 650 °C, followed by a well defined exothermic peak maxima at approximately 800 °C, and a smaller exothermic peak maxima at approximately 920 °C. The endothermic minima corresponds to glass transition while the exothermic peaks correspond to formation of the crystalline phases (crystallization) in the glass.

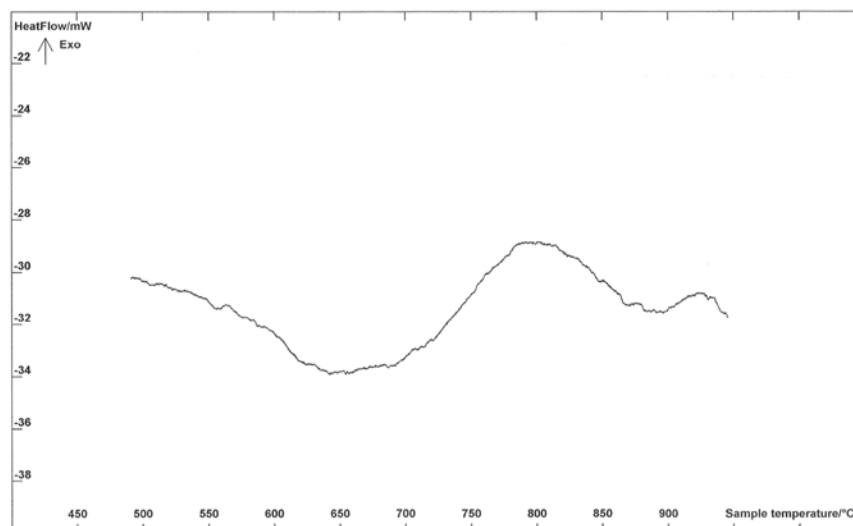


Figure 4.2 DTA thermogram of the glass containing 1 wt% B<sub>2</sub>O<sub>3</sub>.

It is evident that at least two compounds crystallize from this glass during heating. Indeed, as it will be discussed later in Section 4.2.2 more than two crystals were precipitated during crystallization heat treatment of these glasses. There were only minor differences in DTA thermograms of the glasses of different compositions in terms of the endothermic minima and exothermic maxima as will be discussed in Section 4.2.1. It was anticipated that this slight difference in thermal behaviour of glasses did not have such a great influence on that heat treatment temperatures and since they remained the same for all compositions containing different amounts of  $B_2O_3$ . Therefore, it was decided to take a single nucleation temperature as 650 °C and two crystallization temperatures as 850 °C and 1000 °C. The nucleation and growth time were kept constant at 8 hours. Also the heating and cooling rates were kept constant at 3°C/min throughout the heat treatment process.

The colorless as-formed glass pieces of different compositions appeared in white (milky) color after the crystallization heat treatment. It was obvious from the appearance of the crystallized pieces that phase separation occurred during cooling of the glass and at least two crystalline phases precipitated during crystallization of the parent glass. Crystalline phases formed during crystallization of the glass were identified by powder XRD analysis.

Flannery[45] has worked in a mica glass ceramic system containing  $B_2O_3$  and has stated that the outward appearance of the crystallized products is quite similar to that of conventional glass ceramic articles, being opaque and white. The surface quality, especially those compositions containing  $B_2O_3$ , demonstrated satiny finish. After heat treatment, the samples were opacitized. That is, they appeared in white color. It was obvious from the appearance of the blocks that at least two phases crystallized during heat treatment of these glasses. A comparison of the appearance of the glass samples having different amount of  $B_2O_3$  showed that the samples which contained higher amount of  $B_2O_3$  were much whiter and shinier than those contained less amount of  $B_2O_3$ .

## 4.2 ANALYSES

### 4.2.1 Differential Thermal Analysis (DTA)

Glasses of different compositions containing no, 1, 4, and 8 wt% B<sub>2</sub>O<sub>3</sub> were analyzed by DTA as described in Section 3.2.2 to determine the thermal behavior and hence heat treatment temperature for crystallization of these glasses.

The results of DTA were illustrated schematically in Figure 4.2 through Figure 4.5. As seen from the figures there was not a significant difference in DTA thermograms of these glasses with increasing B<sub>2</sub>O<sub>3</sub> additions. DTA thermogram of the glass containing 1 wt% B<sub>2</sub>O<sub>3</sub> indicated that a slight endothermic peak started at about 500 °C and reached the endothermic peak bottom at approximately 650 °C as seen in Figure. 4.2. It raised and ended at approximately 700 °C. Right after this point an exothermic peak, corresponding to crystallization began to form. The exothermic peak turned down at its highest point of 800 °C and ended at approximately 900 °C. Beyond that a development of second exothermic peak was observed. The maxima of the second exothermic peak was at approximately 920 °C. It ended at approximately 950 °C. Melting began at about 1100 °C.

DTA thermograms of the glass containing no B<sub>2</sub>O<sub>3</sub> (the parent glass) indicated that an endothermic peak started at about 600 °C and reached the endothermic peak bottom and curve turned up at 664 °C. Then, the endothermic peak raised and ended at about 760 °C as seen in Figure 4.3. Beyond this point, the exothermic peak, corresponding to crystallization began to form. The exothermic peak turned down at its highest point of 800 °C and ended at approximately 900 °C. Right after this point a second exothermic peak was observed. It ended at 1053 °C. Melting began at about 1150 °C.

DTA thermogram of the glass containing 4 wt% B<sub>2</sub>O<sub>3</sub> indicated that an endothermic peak started at about 600 °C and reached the endothermic peak bottom and curve turned up at 673 °C as seen in Figure 4.4. Then the endothermic peak ended at 700 °C. Beyond this point, the exothermic peak, corresponding to crystallization began to rise. The exothermic peak turned down at its highest point at about 780 °C and ended at approximately 900 °C. After this point, second exothermic peak was observed and it ended at about 1011 °C. Melting began at about 1080 °C.

DTA thermograms of the glass containing 8 wt% B<sub>2</sub>O<sub>3</sub> indicated that an endothermic peak started at about 580 °C and reached the endothermic peak bottom and curve turned up at 635 °C as seen in Figure 4.5. Then, the endothermic peak ended at about 700 °C. Beyond this point an exothermic peak was observed. The maxima of the exothermic peak was at 798 °C. It ended at 892 °C. Beyond this point, a second exothermic peak, corresponding to crystallization began to rise. The exothermic peak turned down at its highest point at about 930 °C. Melting began at about 1050 °C.

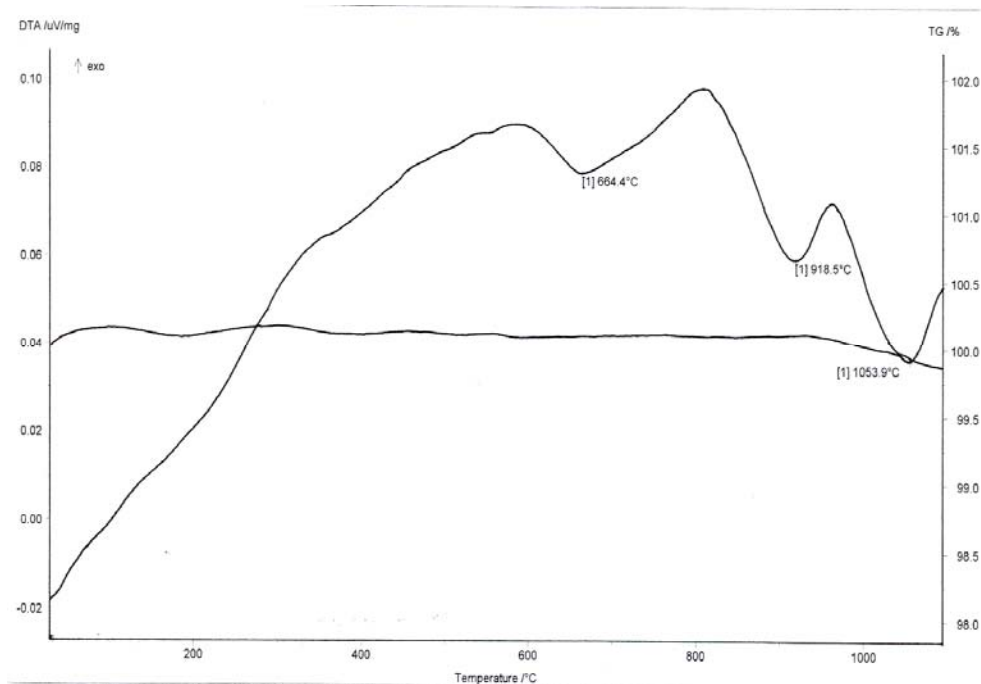


Figure 4.3 DTA thermogram of the glass containing no B<sub>2</sub>O<sub>3</sub>.

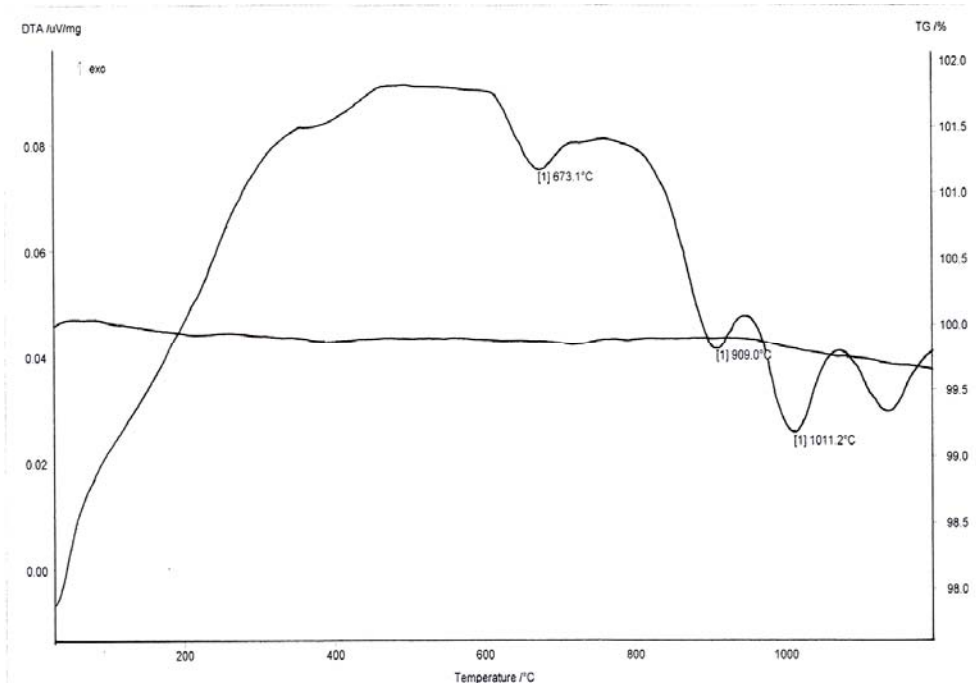


Figure 4.4 DTA thermogram of the glass containing 4 wt%  $B_2O_3$ .

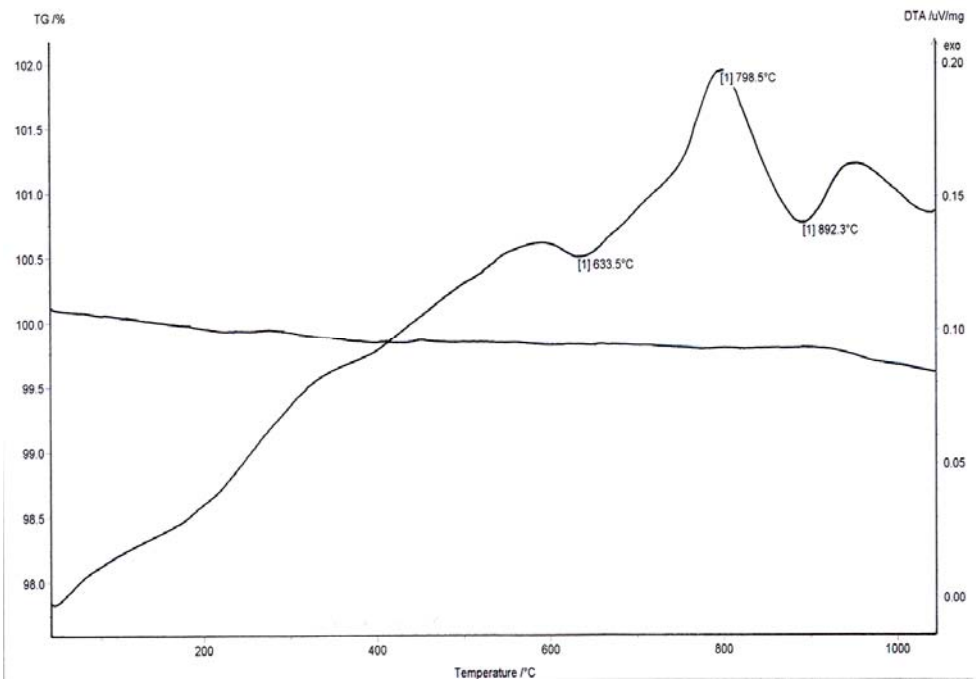


Figure 4.5 DTA thermogram of the glass containing 8 wt%  $B_2O_3$ .

Grossman[51] stated that crystallization temperature should be chosen as a temperature that is very near to melting point. Thus, the maximum crystallization can be obtained. Moreover, it was stated that there is no need to make nucleation to glasses which have slight endothermic peak before crystallization peak on their DTA thermogram[51,52]. It was also stated by Unuma et al.[53] that after 1100 °C the mica crystals convert to cordierite and chondrodite crystals. Therefore, heat treatment should not exceed 1100 °C.

The results of DTA conducted by McMillan[26] on the crystallization of a glass in the MgO-Al<sub>2</sub>O<sub>3</sub>-B<sub>2</sub>O<sub>3</sub> system revealed that conversion of this glass to a glass ceramic could be achieved by a nucleation treatment at 670 °C and a crystallization treatment at 730 °C. He also confirmed that at least two crystalline phases could be precipitated upon crystallization of the glass. Öveçoğlu et al.[54] performed DTA experiments in a temperature range between 25 °C and 1200 °C on a glass of SiO<sub>2</sub>-Al<sub>2</sub>O<sub>3</sub>-MgO-K<sub>2</sub>O-CaO system. The heating rate of 5 °C/min. was chosen as the reference for the nucleation and crystallization temperatures of 735 °C and 870 °C, respectively. Yekta et al.[55] has worked the mica glass ceramic in a SiO<sub>2</sub>-Al<sub>2</sub>O<sub>3</sub>-MgO-K<sub>2</sub>O-B<sub>2</sub>O<sub>3</sub>-F system. They reported that the interval temperature for crystal growth was adopted between 850 °C and 1100 °C. Cheng et al.[56] studied DTA of a mica glass ceramic and reported crystallization temperature range for mica was from 795 °C to 815 °C. Kodaira et al.[11] have conducted DTA on mica glass ceramics and reported that exothermic peak at about 850 °C, as seen in Figure 4.6, indicated the transformation from amorphous state to crystalline fluormica.

James[3] has reported that B<sub>2</sub>O<sub>3</sub> raises the crystallization temperature. However, in this study it was observed that as B<sub>2</sub>O<sub>3</sub> was incorporated into the glass, the glass transition temperature (T<sub>g</sub>) and crystallization temperature decreased. This could be due to a reduced number of bridging bonds in the silica-based network leading to an increase of the viscosity and, consequently, of the glass transition temperature.

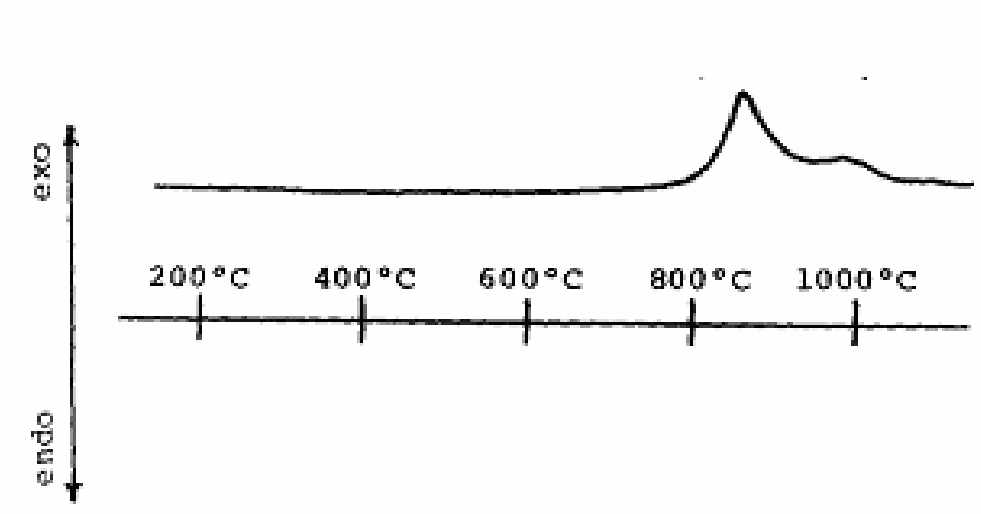


Figure 4.6 DTA analysis of a mica glass ceramic given by Kodaira et al.[11]

## 4.2.2 X – Ray Diffraction (XRD)

The samples containing no, 1, 2, 4 and 8 wt% B<sub>2</sub>O<sub>3</sub> and exposed to different heat treatment were analyzed by XRD to determine and identify the phases precipitated during crystallization. The phases formed in the samples containing 4 and 8 wt% B<sub>2</sub>O<sub>3</sub> were analyzed in two cases; that is, as the lid of the crucible was covered and was not covered during melting. The XRD analysis of the sample containing no B<sub>2</sub>O<sub>3</sub> has suggested that synthetic mica, fluorphlogopite, dehydroxylated muscovite, diopside and wollastonite were precipitated in this glass upon crystallization. Figure 4.7 depicts the XRD traces of samples containing 1, 2, 4 and 8 wt% B<sub>2</sub>O<sub>3</sub> after heat treatment at 650 °C for nucleation and 850 °C for growth. The same crystalline phases as detected in the XRD pattern of the parent glass were developed along with great amount of residual glassy phase. The intensity of the peaks owing to diopside and wollastonite phases increased with increasing amount of B<sub>2</sub>O<sub>3</sub>. The formation of trace amount of sinhalite phase was observed to be precipitated when B<sub>2</sub>O<sub>3</sub> content reached to 8 wt% as seen in Figure 4.7(d).

The chemical formula of the phases precipitated in the glasses investigated are;

Synthetic mica;  $\text{KMg}_3(\text{AlSi}_3\text{O}_{10})\text{F}_2$

Fluorphlogopite;  $\text{KMg}_3(\text{AlSi}_3)\text{O}_{10}\text{F}_2$

Diopside;  $\text{Ca}(\text{MgAl})(\text{SiAl})_2\text{O}_6$

Wollastonite;  $\text{CaSiO}_3$

Dehydroxylated Muscovite;  $\text{KAl}_3\text{Si}_3\text{O}_{11}$

Sinhalite;  $\text{MgAlBO}_4$

Figure 4.8 depicts the XRD traces of samples containing 1, 2, 4 and 8 wt% B<sub>2</sub>O<sub>3</sub> after heat treatment at 650 °C for nucleation and 1000 °C for growth. Again, synthetic mica, fluorphlogopite, dehydroxylated muscovite, diopside and wollastonite precipitated upon crystallization. The intensity of diopside, wollastonite and sinhalite phases became bigger as seen in Figure 4.8.

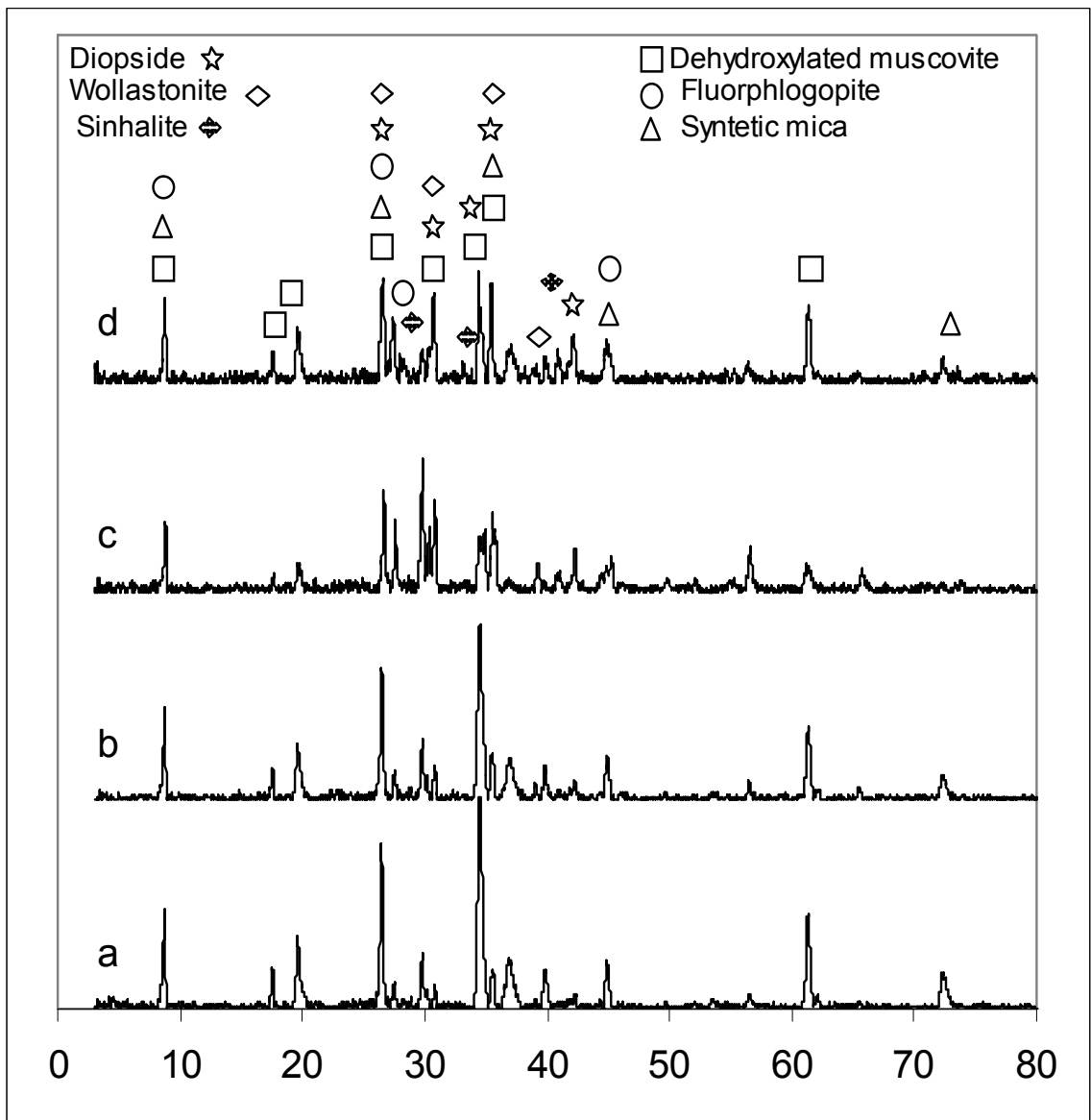


Figure 4.7 The XRD pattern of the glass ceramic samples heat treated at 650 °C for nucleation and at 850 °C for growth. B<sub>2</sub>O<sub>3</sub> content of the samples were;

(a) 1 wt%

(b) 2 wt%

(c) 4 wt%

(d) 8 wt%

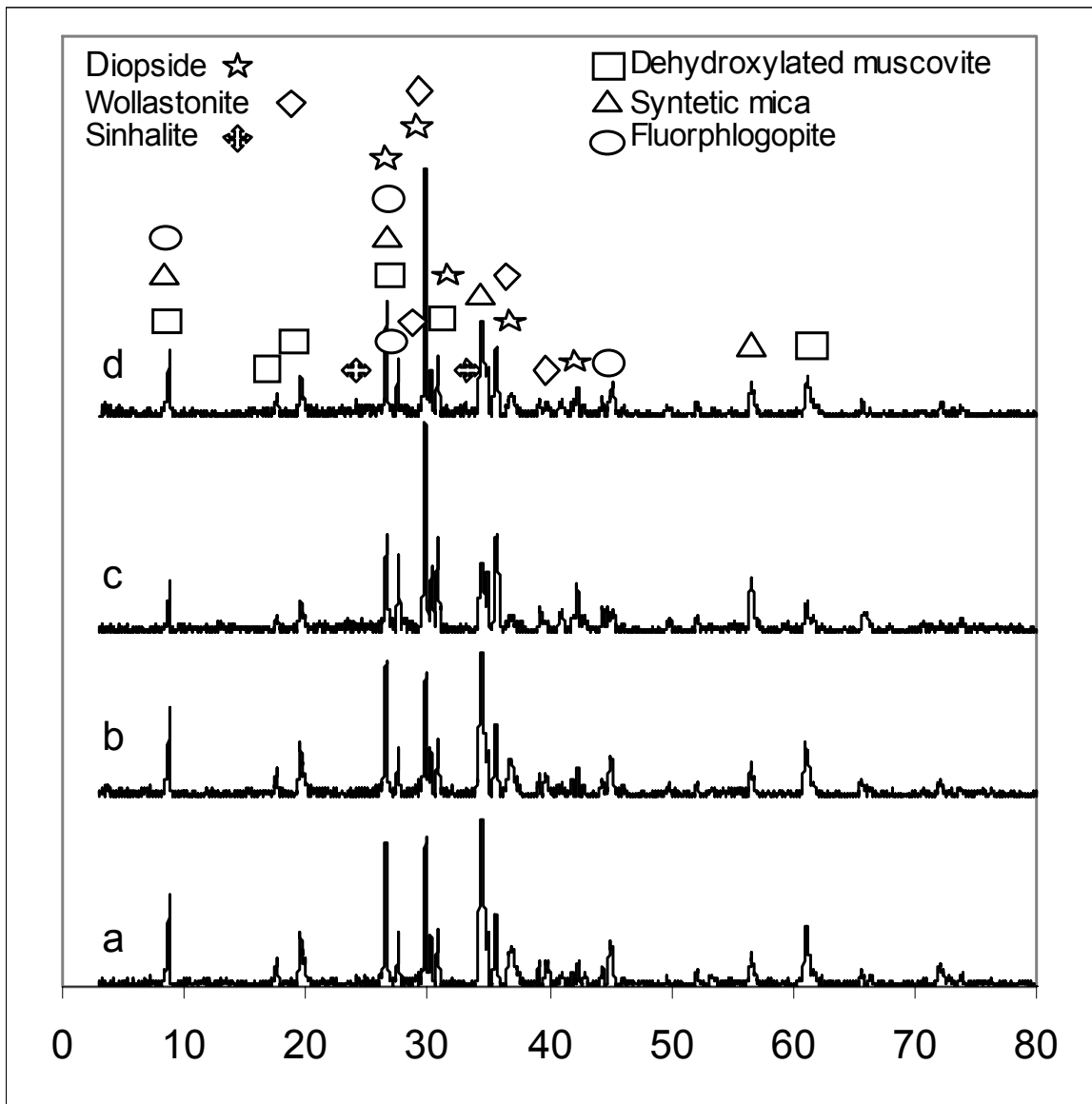


Figure 4.8 The XRD pattern of the glass ceramic samples heat treated at 650 °C for nucleation and at 1000 °C for growth.  $B_2O_3$  content of the samples were;

(a) 1 wt%

(b) 2 wt%

(c) 4 wt%

(d) 8 wt%

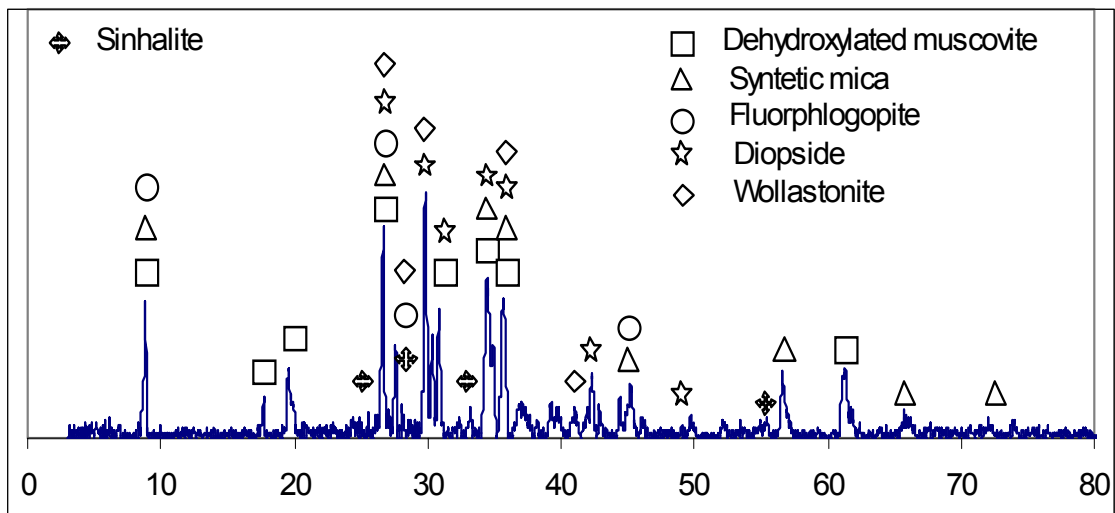


Figure 4.9 The XRD pattern of the sample containing 4 wt%  $B_2O_3$  heat treated at 650 °C for nucleation and at 1000 °C for growth Sample was obtained when the lid of the crucible was closed during melting.

The XRD patterns of the samples containing 4 and 8 wt%  $B_2O_3$  heat treated at 650 °C for nucleation and at 1000 °C for crystal growth were shown in Figure 4.9 and Figure 4.10, respectively. Samples were obtained when the lid of the crucible was closed during melting According to these figures, the same crystalline phases, i.e., diopside, synthetic mica, fluorphlogopite, dehydroxylated muscovite and wollastonite were precipitated. However, the main difference between these two patterns with the patterns of the samples containing same amount of  $B_2O_3$  and exposed to the same heat treatment but obtained when the lid of the crucible was open during melting was that, the intensity of the sinhalite phase which precipitated in both of the samples was higher. Sinhalite was not observed in the sample containing 4 wt%  $B_2O_3$  heat treated at 650 °C for nucleation and at 1000 °C for crystal growth was shown in Figure 4.8(c).

Vogel et al.[25] have reported that the well known glass-ceramic Bioverit<sup>®</sup>, which contains muscovite and fluorapatite, has been successfully used in clinical applications for many years since it exhibits both excellent machinability and high bioactivity. However in this study fluorapatite were not detected through XRD analysis although muscovite phase was observed as dehydroxylated muscovite. The reason why fluorapatite was not observed is attributed to the absence of P<sub>2</sub>O<sub>5</sub> in batch composition. It is known that apatite phase is formed only when P<sub>2</sub>O<sub>5</sub> is present in the system.

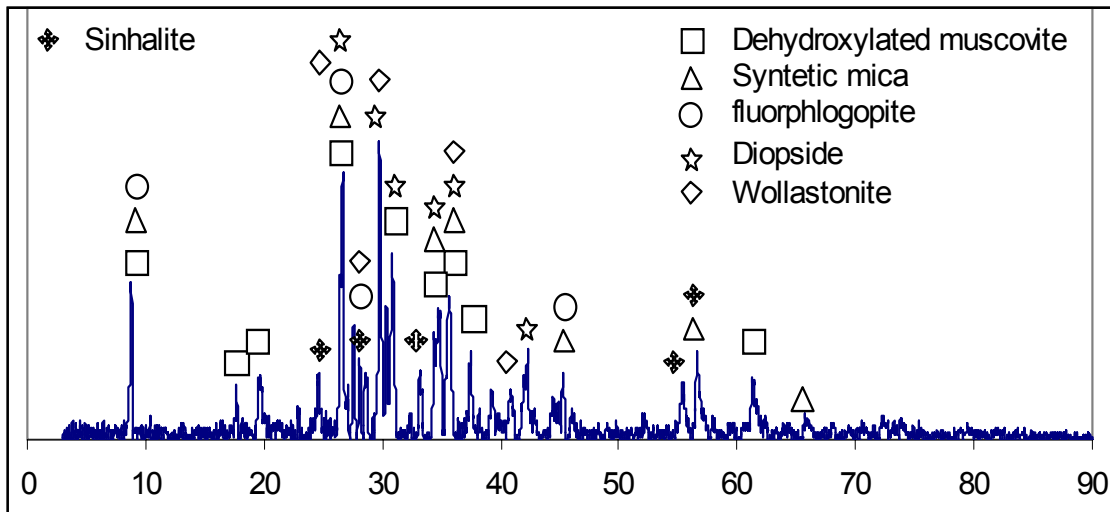


Figure 4.10 The XRD pattern of the sample containing 8 wt% B<sub>2</sub>O<sub>3</sub> heat treated at 650 °C for nucleation and at 1000 °C for growth. Sample was obtained when the lid of the crucible was closed during melting.

Der[13] has reported that the XRD analysis of the mica glass ceramic suggested the formation of the phases, mostly Leucite (KAlSi<sub>2</sub>O<sub>6</sub>) and K<sub>2</sub>MgSi<sub>5</sub>O<sub>12</sub> on the surface of the sample. However, the XRD pattern taken from the bulk of the sample suggested that mostly fluorphlogopite crystals were formed. Öveçoğlu et al.[54] studied XRD of the glass ceramic and found that the major crystalline phase was diopside-aluminan phase as seen in Figure 4.11. They concluded that the crystallization temperature of diopside was at 1000 °C. The present

study confirms the findings of Öveçoğlu et al.[54]. Taira and Yamaki[57] have characterized the nine mica glass ceramics. Five contained layered mica in a matrix glassy phase, two others consisted of mica with interconnected diopside crystals showed considerable intercrystal porosity.

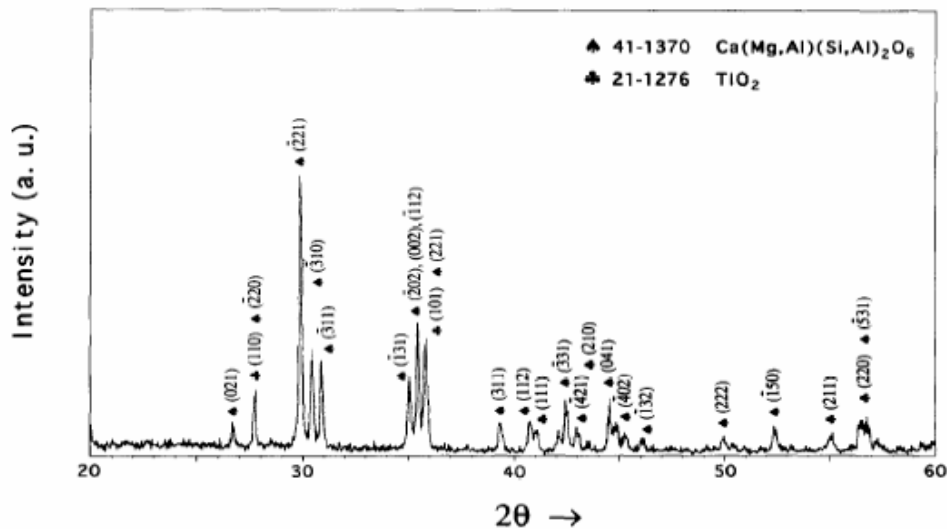


Figure 4.11 XRD pattern of the diopside-based glass ceramic given by Öveçoğlu et al.(54)

Tulyaganov et al.[58] have worked in a mica glass ceramic system and reported that the phases formed in the system with respect to the results of the XRD analysis. They observed that tetrasilicic mica was formed at 700 °C and diopside started to precipitate at 800 °C. Diopside were regularly crystallized at 945 °C.

Tzeng et al.[8] investigated the four mica glass ceramic products, which are marketed under the commercial name DICOR<sup>®</sup>, and reported that the phases precipitated are synthetic mica crystals with a structure similar to fluorphlogopite and boronfluorphlogopite. Although synthetic mica was observed in this present study, boronfluorphlogopite was not observed. The reason why boronfluorphlogopite was not observed is not known at the moment. But

increasing boron content increased the fluorine evaporation and caused a decrease in fluorine content of the glass.

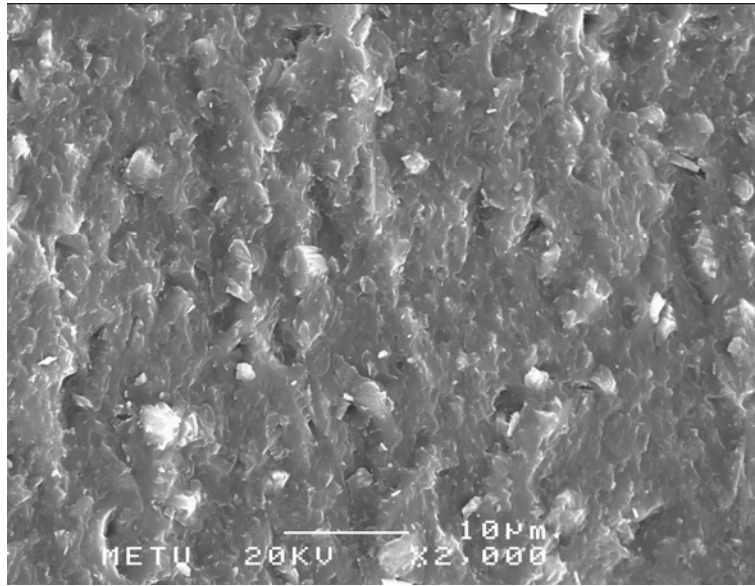
Beall[1] has reported that the glass compositions containing more than 5 wt%  $B_2O_3$ , fluoroborite,  $Mg_3BO_3F_3$  is the crystal phase to precipitate. However, in the present study, fluoroborite was not observed to form instead; the sinhalite phase was observed with increasing  $B_2O_3$  content.

There is not any detailed information about the formation of sinhalite phase from these glasses in the literature. Sinhalite,  $MgAl[BO_4]$ , with an olivine structure and tetrahedral boron is part of the system  $MgO-Al_2O_3-B_2O_3$ (MAB). It is stable at 1 atm up to 1075 °C[59] and has been synthesized at pressures as high as 80 kbar and 1000 °C[60]. In the hydrous system MABH the appearance of another phase remarkably similar to sinhalite in its physical properties was recently recognized by Krosse et al.[61]. Therefore, it was given in the preliminary name 'pseudosinhalite'. Its composition is, however, more aluminous than sinhalite and very close to the join sinhalite-corundum with a chemical formula of  $MgAlBO_4$ . Based on the crystal structure determined by Daniels (see Krosse et al.[61]), 'pseudosinhalite' exhibits hexagonal close oxygen packing like sinhalite, but with a different occupation scheme of octahedral and tetrahedral sites. Its pressure and temperature stability determined by Krosse[62] and reported in the review by Werding and Schreyer[63] extends from low pressures up to 40 kbar, at 950 °C. At higher temperatures, along a rather flat dehydration curve, 'pseudosinhalite' breaks down to form sinhalite+corundum+ $H_2O$ . It may well be that 'pseudosinhalite' also occurs as a mineral in nature; indeed it may have been misidentified as sinhalite in the past. At any rate, these two aluminous borate phases containing tetrahedral boron are remarkably stable at high pressures and may fractionate boron in natural rocks, provided they can coexist with silicates. This is confirmed for natural occurrences of sinhalite by Grew et al.[64] and experimentally by the work of Werding et al.[59], who reported products containing sinhalite together with forsterite and probably a tourmaline phase.

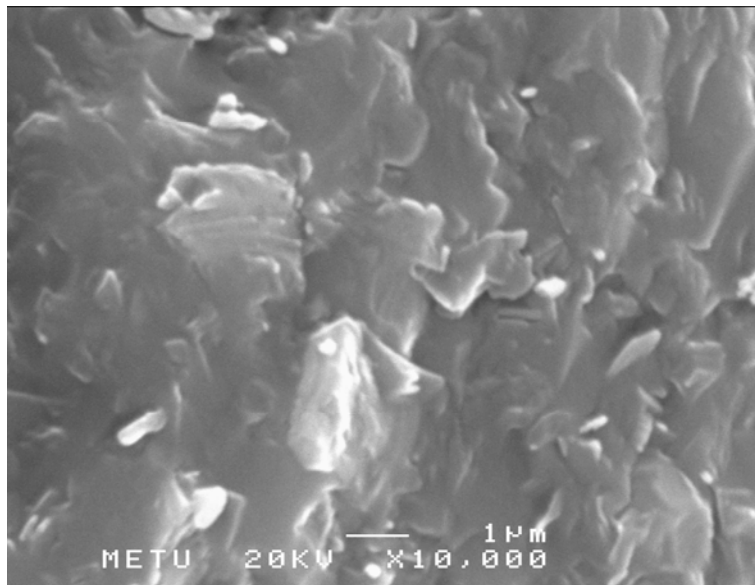
It is not clearly known the effect of sinhalite to the glass ceramics or mica glass ceramics in the literature. According to the information given above it positively affects the mica glass ceramics with respect to the machinability due to the extension of sinhalite from low pressure at low temperatures to the higher temperatures.

### **4.2.3 Scanning Electron Microscope (SEM)**

The samples containing 1, 2, 4 and 8 wt%  $B_2O_3$  and exposed to different heat treatment were analyzed by SEM to observe the microstructure developed with increasing  $B_2O_3$  content. SEM images of the sample containing 1 wt%  $B_2O_3$  heat treated at two different crystallization conditions were shown in Figure 4.12 and Figure 4.13. Figure 4.12 is the SEM micrograph for the sample heat treated at 650 °C for nucleation and at 850 °C for growth while Figure 4.13 is the SEM micrograph for the sample heat treated at 650 °C for nucleation and at 1000 °C for growth. The microstructure of the samples exhibited flake-like shaped crystals in a residual glassy matrix. The sizes of the grains for the sample crystallized at 850 °C were smaller than that of the grains for the sample crystallized at 1000 °C. There exists lamellar mica phases in the microstructure of both samples. Although the crystalline size was too small to be observed clearly from Figure 4.12, the flake-like mica crystals can be observed easily in Figure 4.13.



(a)

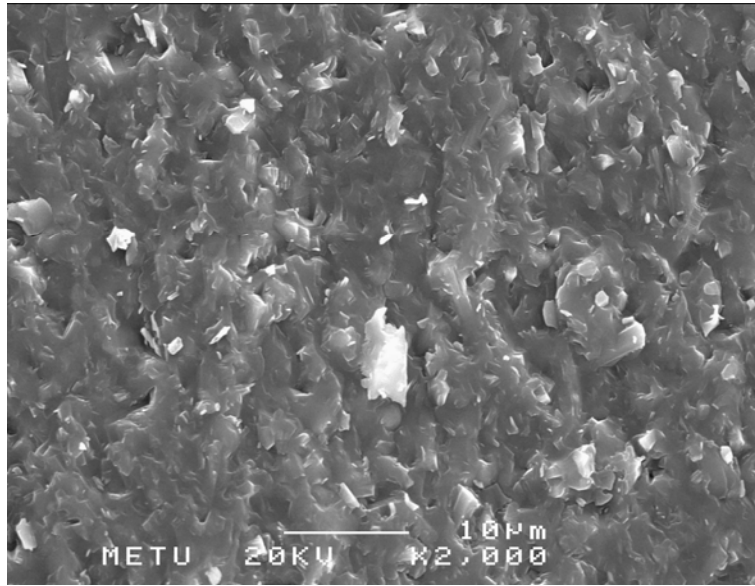


(b)

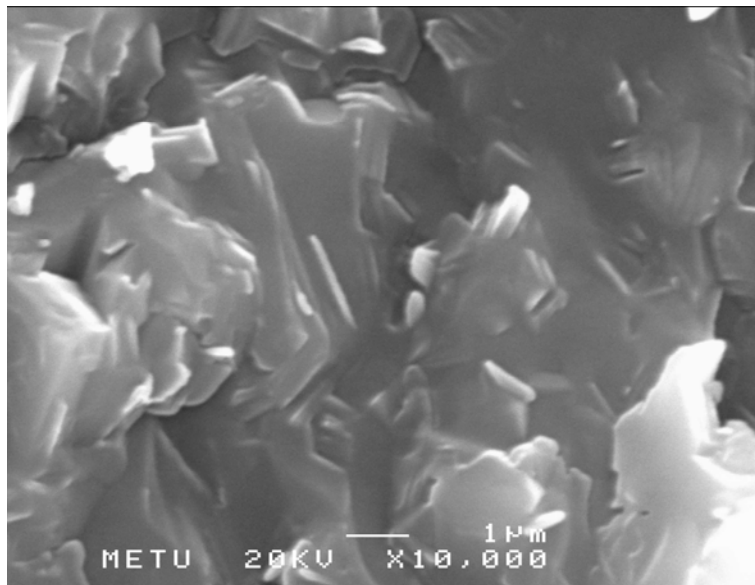
Figure 4.12 SEM micrographs of a glass ceramic sample containing 1 wt%  $B_2O_3$ . The sample was heat treated at 650 °C for nucleation and at 850 °C for crystal growth and was obtained when the lid of the crucible was open during melting.

(a) X 2000

(b) X 10000



(a)



(b)

Figure 4.13 SEM micrographs of a glass ceramic sample containing 1 wt%  $B_2O_3$ . The sample was heat treated at 650 °C for nucleation and at 1000 °C for crystal growth and was obtained when the lid of the crucible was open during melting.

(a) X 2000

(b) X 10000

Vogel et al.[25] have worked on a  $K_2O$ - $MgO$ - $Al_2O_3$ - $SiO_2$ - $CaO$  and F glass ceramic system and detected the fluorphlogopite crystals. They observed flat, flake-like shaped fluorphlogopite crystals as seen in Figure 4.14. A comparison made between Figure 4.13(a) and Figure 4.14 revealed that similar morphology was observed on the mica glass ceramics studied in this investigation.

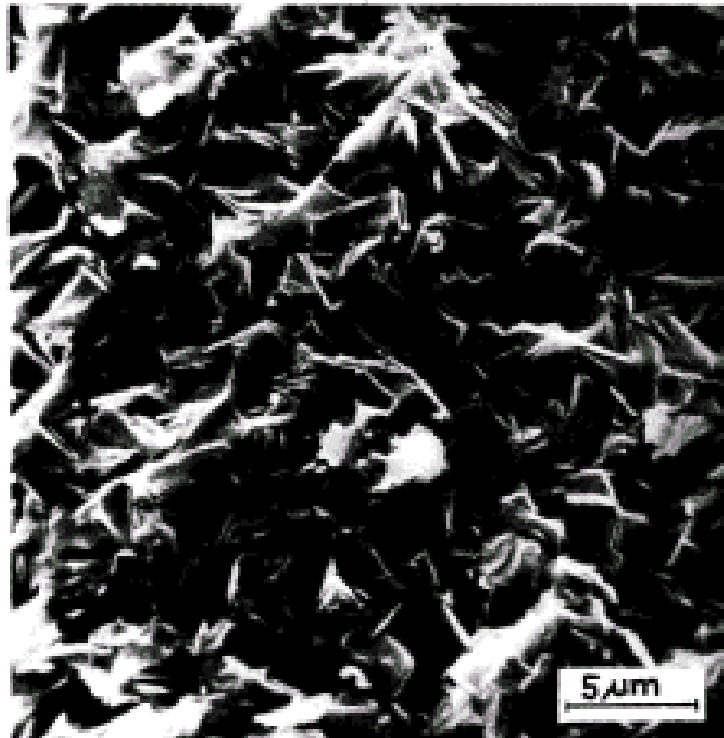
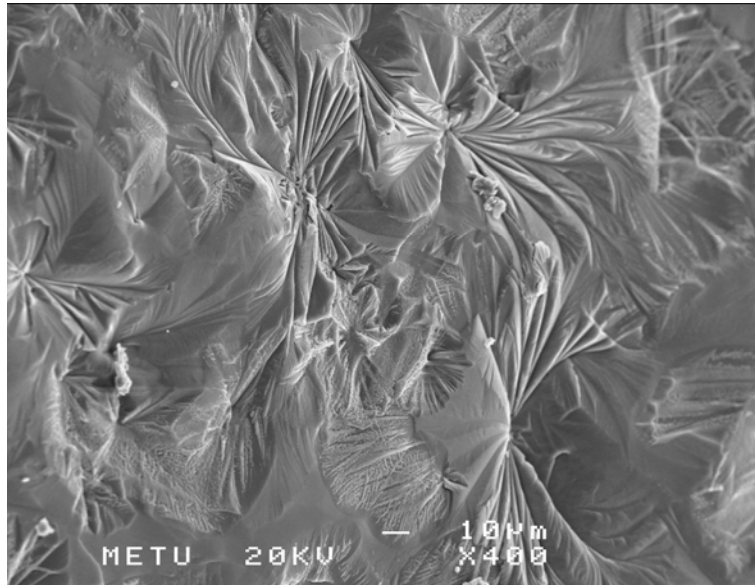


Figure 4.14 SEM micrograph of the machinable glass ceramic with flat, flake-like, fluorphlogopite crystals given by Vogel et al.[25].

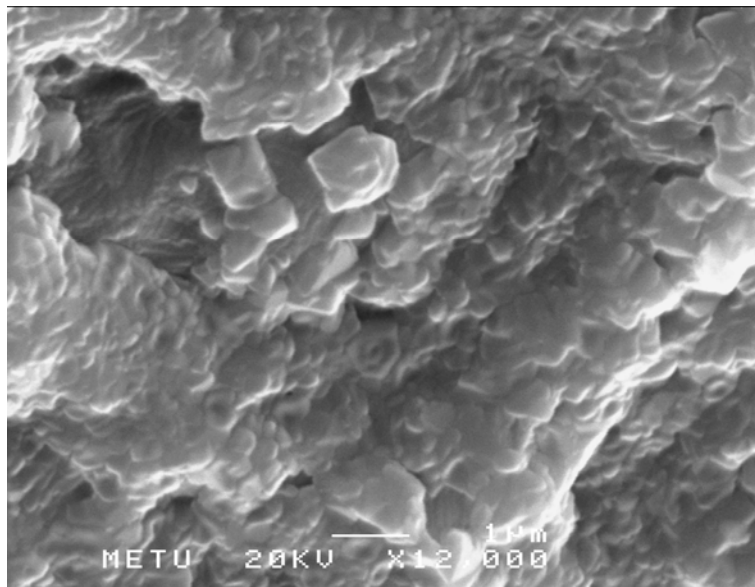
The micrographs of the glass ceramic sample containing 2 wt% B<sub>2</sub>O<sub>3</sub> heat treated at 650 °C for nucleation and 850 °C for crystal growth show the start of the development of diopside as star-like skeletal, feathery growths and hexagonal markings in cryptocrystalline base as seen in Figure 4.15(a). Grains and their size were not determined clearly. This type of crystals were observed mostly in the glass ceramic system containing diopside crystals. Diopside, when crystallized, was usually developed in minor amounts at temperatures around 850 °C[65]. Shennawi et al.[65] has worked on a mica glass ceramic system and observed a concomitant development of diopside as star-like, skeletal growth. Hexagonal markings took place as seen in Figure 4.16. The microstructure shown in Figure 4.15(a) resembles very much to this microstructure.

The SEM image of the same sample at higher magnification exhibited crystals of average size about 0.3–0.4 μm as shown in Figure 4.15(b). The microstructure was uniform and porosities between the grains were apparent. As discussed in section 4.2.2, the observed grains should belong to fluorphlogopite, synthetic mica, and diopside.

The microstructure of the sample containing 2 wt% B<sub>2</sub>O<sub>3</sub> heat treated at 650 °C for nucleation and at 1000 °C for growth was shown in Figure 4.16. Diopside crystals have been observed like a donut. The outer dimension of the grains were about 0.8–0.9 μm. Porosities between and in the grains were apparent. Similar morphology has been reported for glasses which contained apatite and phlogopite, where large spheres and small droplets enriched in Mg, Al, Na, K and F were embedded in glass silicate matrix[66]. Most likely, the tendency of glasses with relatively high volume fraction of diopside and fluorphlogopite to favour phase separation as well as the formation of large spherical droplets caused strong opacity effect (light scattering) resulting in the milky appearance.



(a)



(b)

Figure 4.15 SEM micrographs of a glass ceramic sample containing 2 wt%  $B_2O_3$ . The sample was heat treated at 650 °C for nucleation and at 850 °C for crystal growth and was obtained when the lid of the crucible was open during melting.

(a) X 400

(b) X 12000

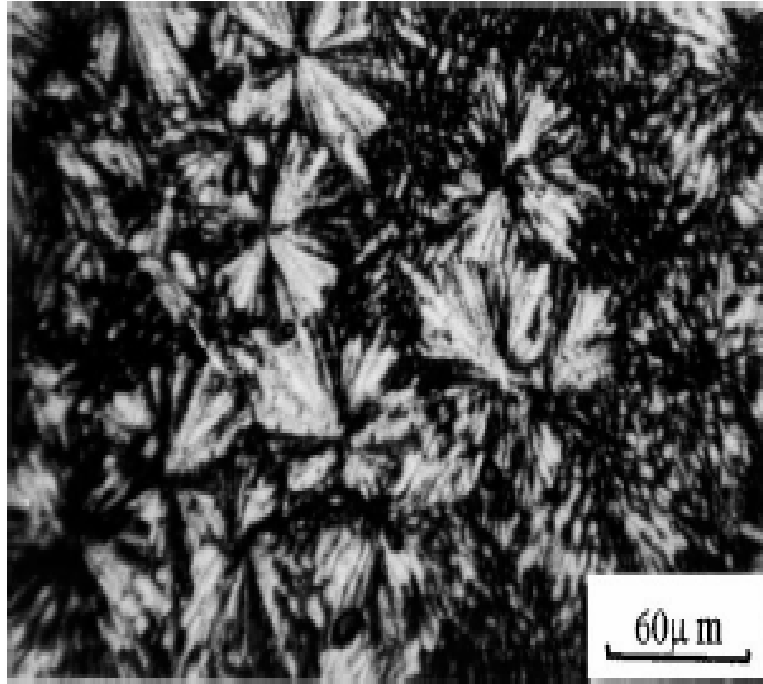
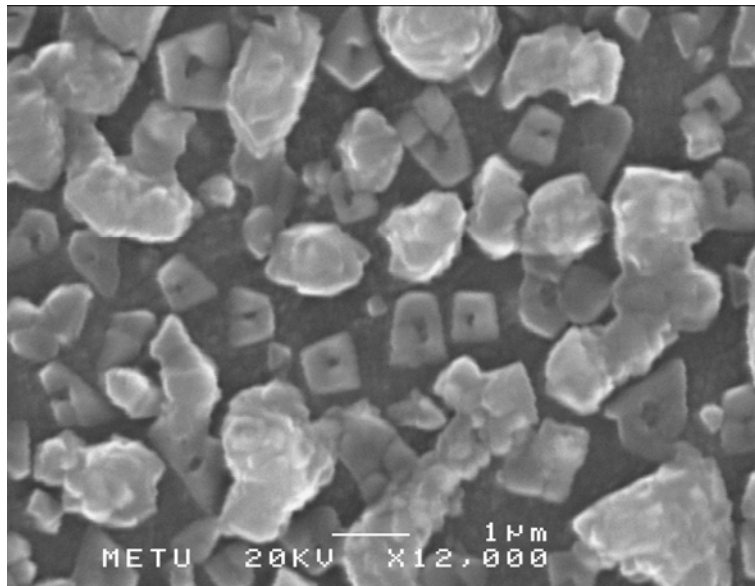
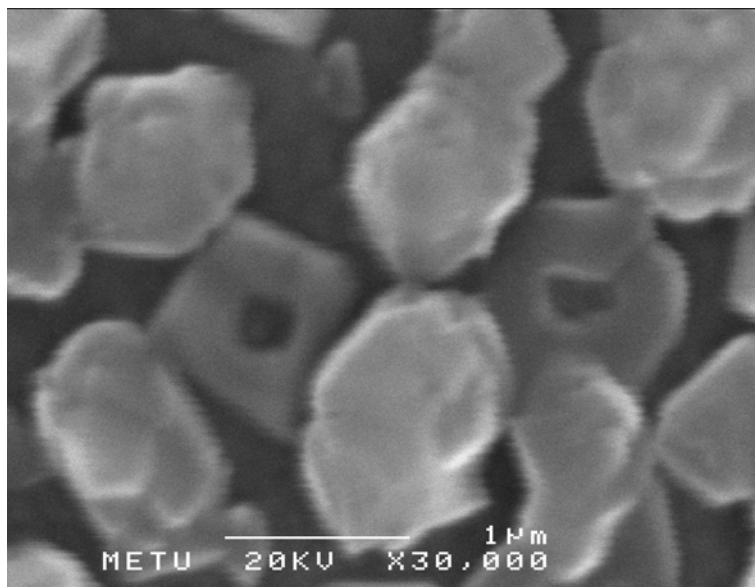


Figure 4.16 SEM micrograph of the sample star-like, skeletal diopside growth given by Shennawi et al.[65] X 500.



(a)



(b)

Figure 4.17 SEM micrographs of a glass ceramic sample containing 2 wt%  $B_2O_3$ . The sample was heat treated at 650 °C for nucleation and at 1000 °C for crystal growth and was obtained when the lid of the crucible was open during melting.

(a) X 12000

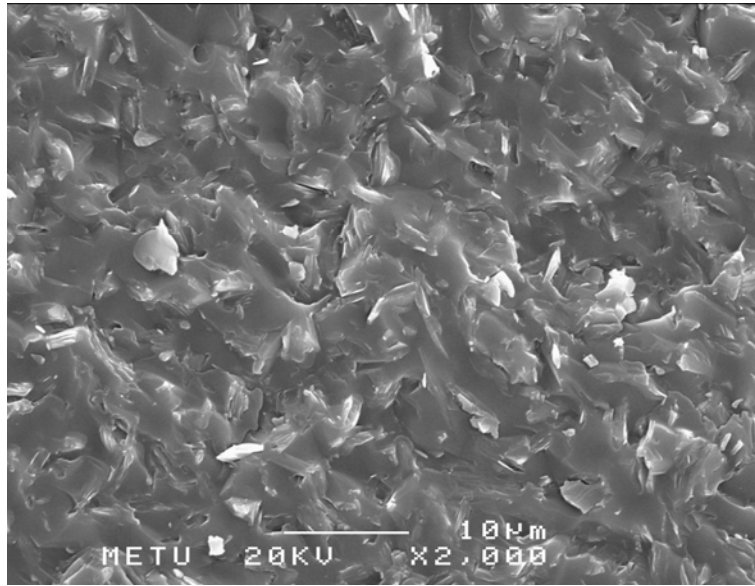
(b) X 30000

The representative microstructure of the glass ceramic sample containing 4 wt% B<sub>2</sub>O<sub>3</sub> heat treated at 650 °C for nucleation and at 850 °C for crystal growth as seen in Figure 4.18. The sample was obtained when the lid of the crucible was open during melting. The resulting microstructures were uniform and involved small and randomly distributed crystals and small amount of porosity between the crystals. It was even more difficult to estimate the nature of the crystals, but according to XRD analysis as seen in Figure 4.7(c) the observed grains should belong to diopside, synthetic mica, fluorphlogopite and wollastonite.

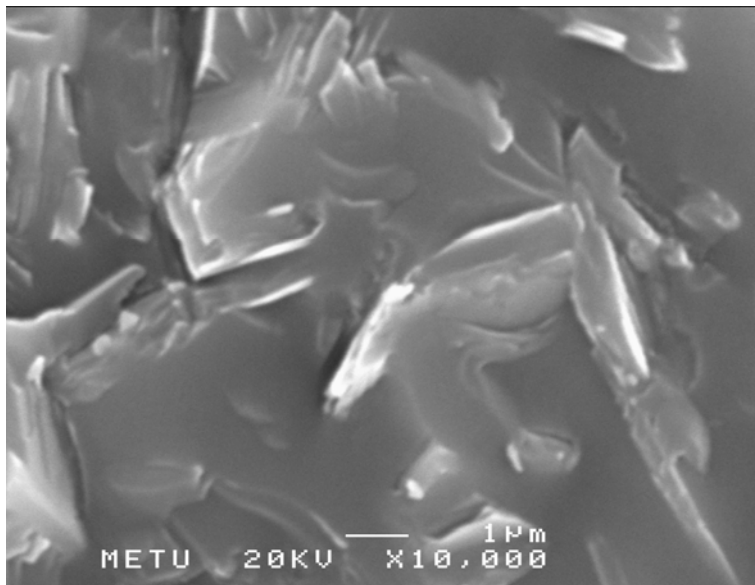
The SEM micrographs of the sample with the same composition but heat treated at 650 °C for nucleation and at 1000 °C for growth was shown in Figure 4.19. The microstructure illustrated the flake like crystals with glassy matrix. The microstructures were uniform and involved small amount of porosity between the crystals.

Typical SEM micrographs of the mica glass ceramic sample containing 4 wt% B<sub>2</sub>O<sub>3</sub> heat treated at 650 °C for nucleation and at 1000 °C for growth is shown in Figure 4.20. The samples were obtained when the lid of the crucible was closed during melting. The micrograph indicated the flake like crystals from an initial base. As seen in Figure 4.20(a), the length of the crystals ranged between 5 and 10 μm.

Taira and Yamaki[59] have investigated two wollastonite based crystals with considerable intercrystal porosity and they concluded that cleavage of layered structures and pre-existing microcracks provide the ceramics with excellent machinability. Ease in cutting and resistance of machinability were related to the amount of crystallinity and porosity. In general, it appears that the more crystalline and porous the ceramic, the weaker and more machinable it becomes.



(a)

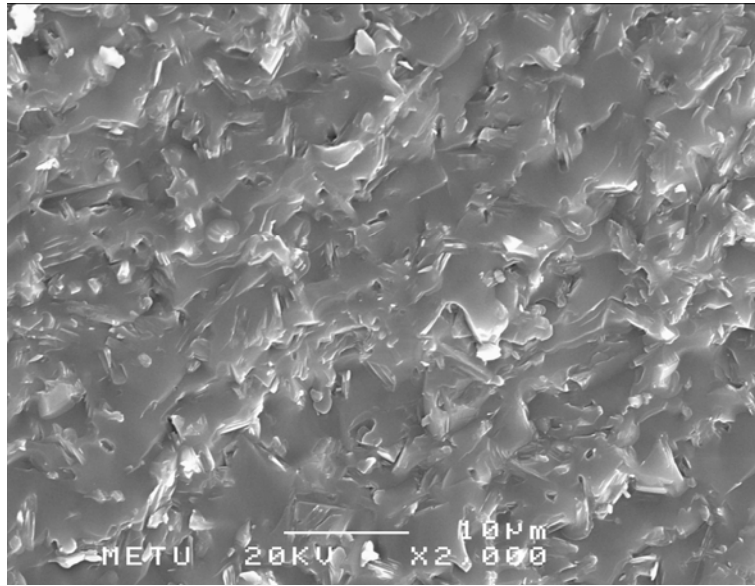


(b)

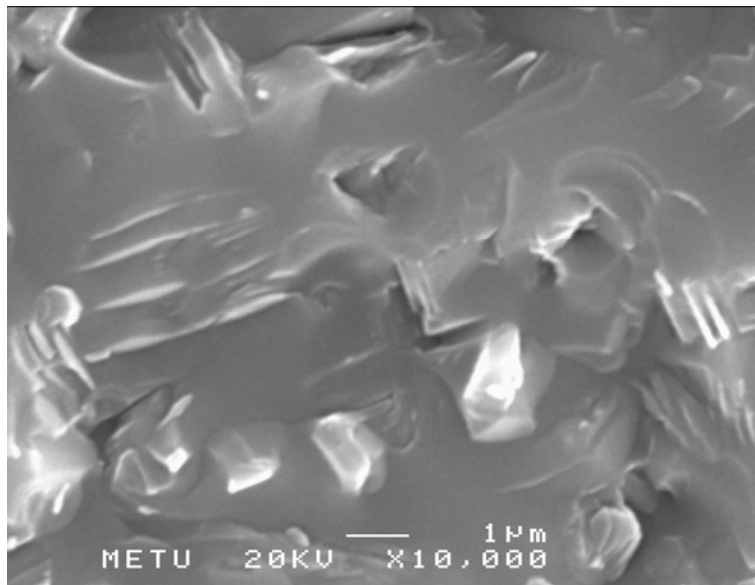
Figure 4.18 SEM micrographs of a glass ceramic sample containing 4 wt%  $B_2O_3$ . The sample was heat treated at 650 °C for nucleation and at 850 °C for crystal growth and was obtained when the lid of the crucible was open during melting.

(a) X 2000

(b) X 10000



(a)

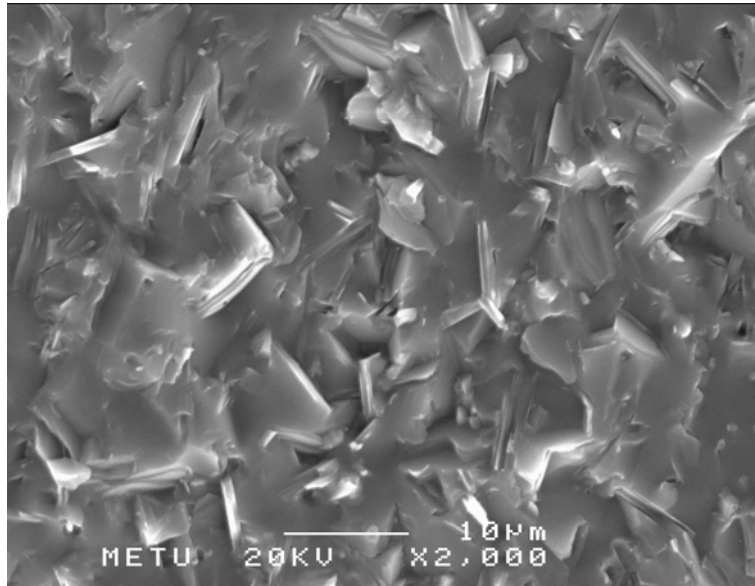


(b)

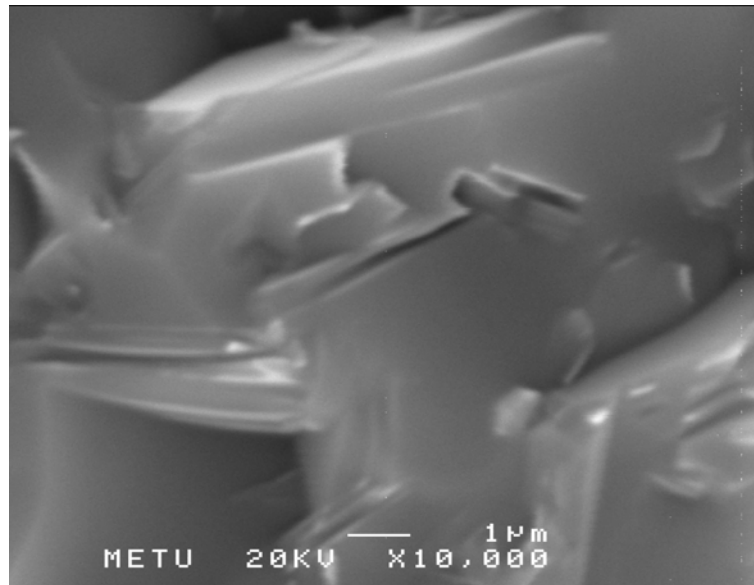
Figure 4.19 SEM micrographs of a glass ceramic sample containing 4 wt%  $B_2O_3$ . The sample was heat treated at 650 °C for nucleation and at 1000 °C for crystal growth and was obtained when the lid of the crucible was open during melting.

(a) X 2000

(b) X 10000



(a)



(b)

Figure 4.20 SEM micrographs of a glass ceramic sample containing 4 wt%  $B_2O_3$ . The sample was heat treated at 650 °C for nucleation and at 1000 °C for crystal growth and was obtained when the lid of the crucible was closed during melting.

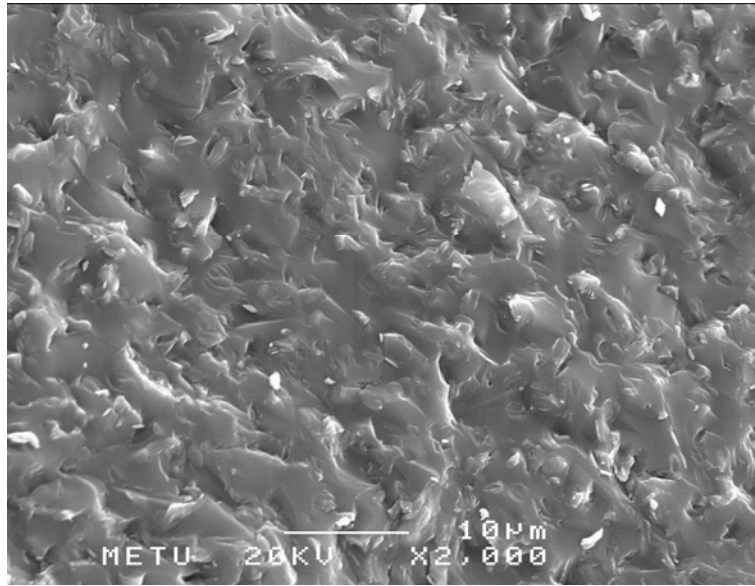
(a) X 2000

(b) X 10000

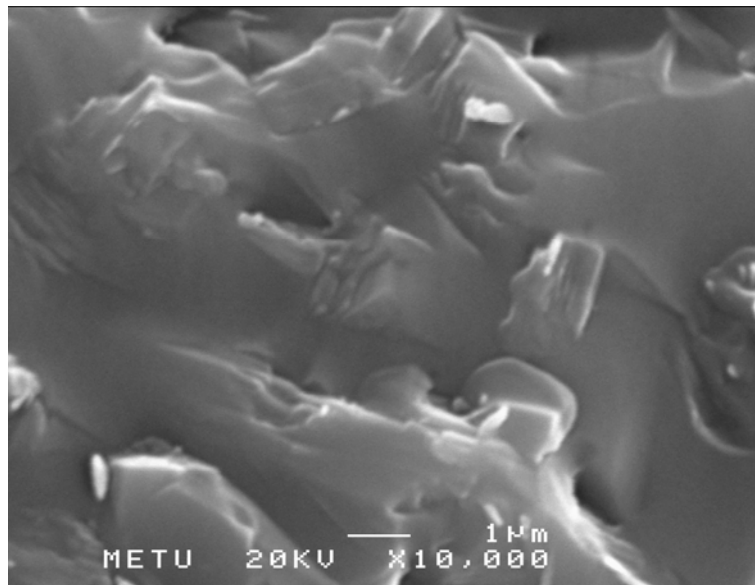
The representative microstructures of the sample containing 8 wt% B<sub>2</sub>O<sub>3</sub> heat treated at 650 °C for nucleation and at 1000 °C for growth, and at 650 °C for nucleation and at 1000 °C for growth were shown in Figure 4.21 and Figure 4.22, respectively. Typical structure of randomly oriented interlocked mica crystals was observed in both samples. The dense structure comprised interlocked almost spherical and ellipsoid crystals, most likely nucleated from the separated droplets and observed in the parent glasses. Owing to the low intensity of diopside and wollastonite peaks in the XRD spectra shown in Figure 4.7(d), the crystals observed, were mostly fluorophlogopite and synthetic mica.

The microstructure of the sample containing 8 wt% B<sub>2</sub>O<sub>3</sub> heat treated at 650 °C for nucleation and at 1000 °C for growth was shown in Figure 4.23. The sample was obtained when the lid of the crucible was closed during melting. SEM micrographs of the samples were taken respectively, from crystal-rich and glass-rich regions showing the conical rod-like and flake-like crystals fanning out from an initial base. A qualitative EDX analysis on several crystals, as will be discussed in Section 4.2.4, suggested that they were diopside and fluorophlogopite. The length of crystals ranges between 10 and 15 μm. In addition, diopside and fluorophlogopite crystals looked like brooms embedded in the parent glass matrix. Further, their clustering suggested that they seemed to have grown together in a bundle. Overall, the morphology, orientation and size of these crystals indicated that surface crystallization took place in only one preferred orientation.

B<sub>2</sub>O<sub>3</sub> is a glass former. When B<sub>2</sub>O<sub>3</sub> was added to the batch, it increased the glassy phase in the samples as seen obviously from the SEM micrographs investigated in this thesis. The pores in the donut like grains, as seen in Figure 4.17 could be the result of increasing temperature and B<sub>2</sub>O<sub>3</sub> content.



(a)

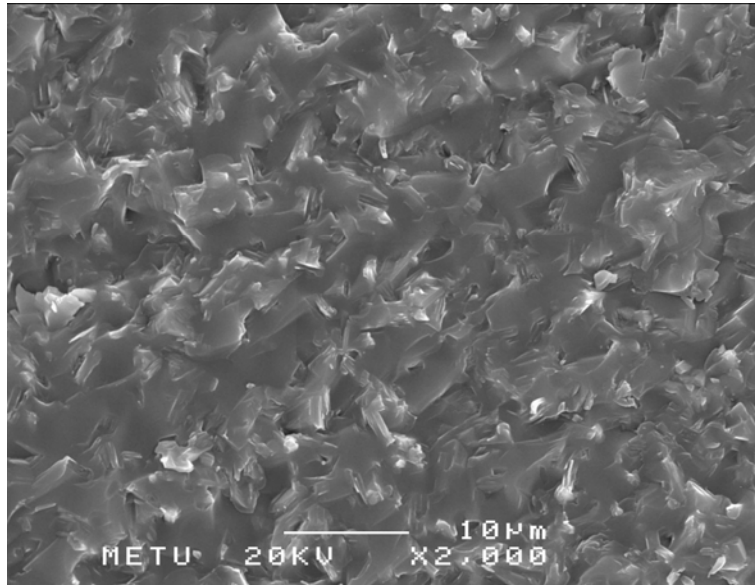


(b)

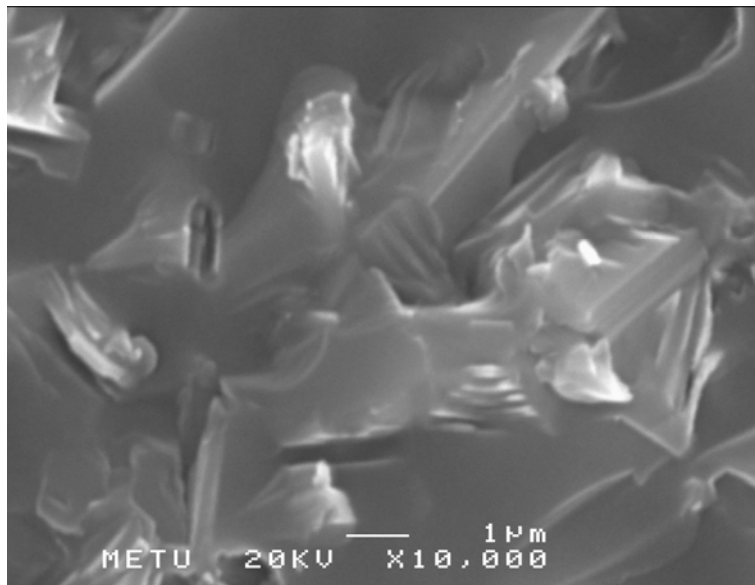
Figure 4.21 SEM micrographs of a glass ceramic sample containing 8 wt%  $B_2O_3$ . The sample was heat treated at 650 °C for nucleation and at 850 °C for crystal growth and was obtained when the lid of the crucible was open during melting.

(a) X 2000

(b) X 10000



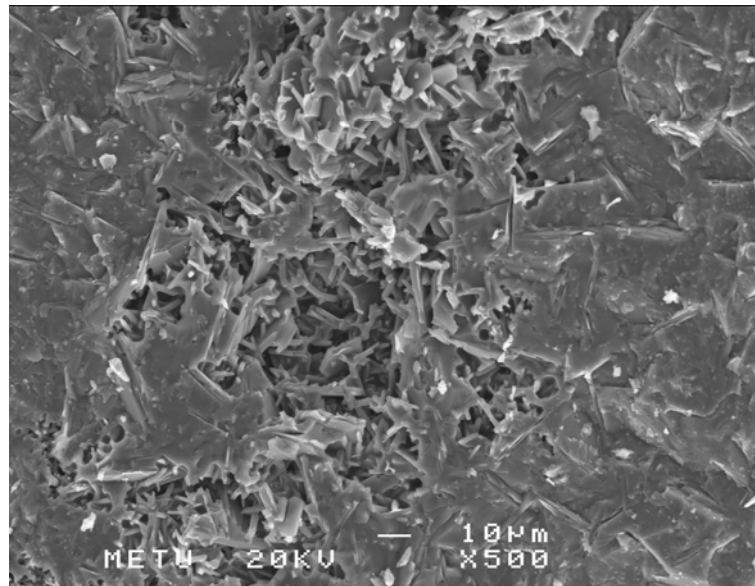
(a)



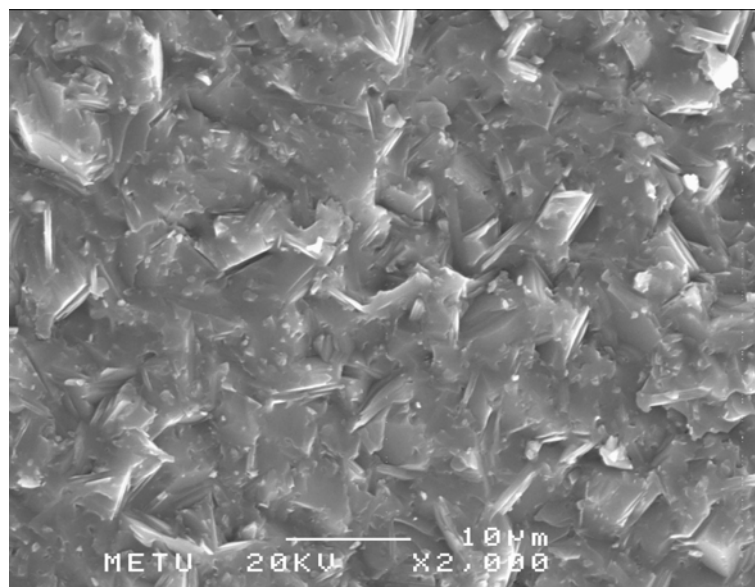
(b)

Figure 4.22 SEM micrographs of a glass ceramic sample containing 8 wt%  $B_2O_3$ . The sample was heat treated at 650 °C for nucleation and at 1000 °C for crystal growth and was obtained when the lid of the crucible was open during melting.

(a) X 2000 (b) X 10000



(a)



(b)

Figure 4.23 SEM micrographs of a glass ceramic sample containing 8 wt%  $B_2O_3$ . The sample was heat treated at 650 °C for nucleation and at 1000 °C for crystal growth and was obtained when the lid of the crucible was closed during melting.

(a) X 500 (b) X 2000

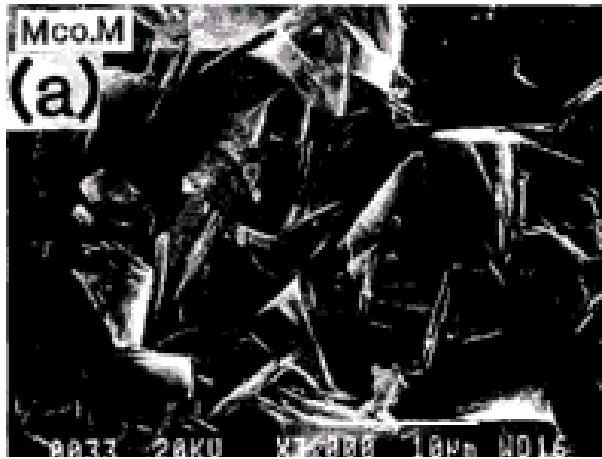
Hench[19] has reported that the potential advantage offered by a porous ceramic implant is the mechanical stability of the highly convoluted interface developed when bone grows into the pores of the ceramic. The two primary applications are the use of Hydroxyapatite coating on the porous surfaces of total joint prostheses as an alternative to cement fixation and as coatings on dental implants to achieve bioactive fixation and use of porous synthetic calcium phosphate ceramics to fill bone defects. A porous implant serves as structural bridge and model or scaffold for bone formation. The rate of the bone growth was accelerated by the porous bioactive ceramics, and also strength of the bone-implant interface was enhanced. Therefore formation of small amount of porosity between and in the grains might be an advantage in terms of bioactivity for biological applications.

Tzeng et al.[8] investigated the four mica glass ceramic products, which were marketed under commercial name DICOR<sup>®</sup>, and stated that the fracture surface gave evidence of the fracture path. Ladder-like flakes existed in the upper portion of the sample under SEM, which resulted from the fracture path across the interface between glass and abnormal grains. In addition to weak interface, cleavage planes of mica crystals also led to easy fracture propagation, especially for large grains. Porosity exhibited fracture propagation along the cleavage plane of mica crystal. Combination of easy fracture propagation along cleavage planes of mica crystals and weak interfaces between glass matrix and mica grains, especially for abnormal grain and the grain which has porosity, resulted in the lower strength and excellent machinability in samples. The observed microstructure in the mica glass ceramics studied concomitate with this explanation.

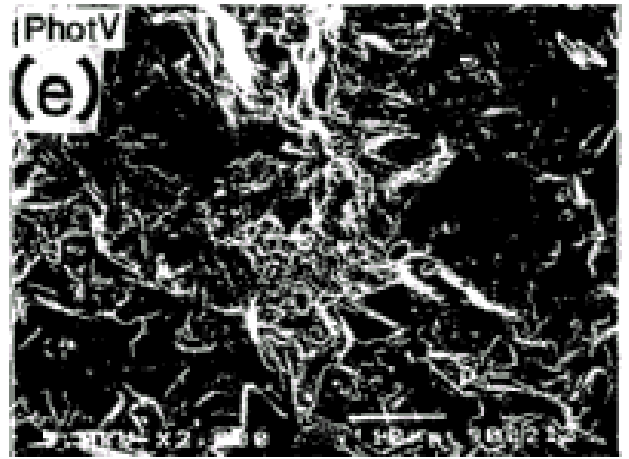
Salama and Darwish[66] have reported that the diopside causes the formation of pores or voids on the surface. During the SEM observation in this thesis work the formation of pores or voids have been observed in and among the grains.

Taira and Yamaki[26] have characterized the nine mica glass ceramics, which marketed under different commercial name. According to SEM analysis of the nine machinable glass ceramics, three of them showed the same morphology with the samples have been studied in this thesis work. The samples owning to Macor-M<sup>®</sup>, Photoveel<sup>®</sup> and Machinax<sup>®</sup> had the similar micrographs as seen in Figure 4.24. Macor<sup>®</sup> and Photoveel<sup>®</sup> contained only mica crystals, however Machinax<sup>®</sup> contained wollastonite and diopside crystals. They stated that Macor-M<sup>®</sup> contained two dimensional mica crystals in a brittle glass matrix. During cutting, the cleavage of mica crystals localized fracture of the glass on a microscopic scale and allowed powdered chips to form easily, gave rise to good machinability.

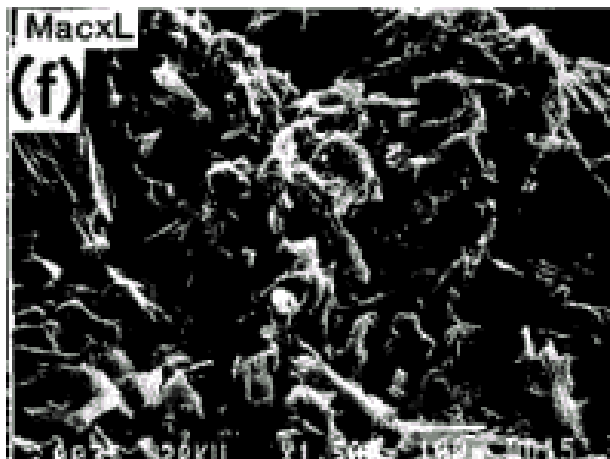
Beall[1] has prepared mica glass ceramics with 3-15 wt% B<sub>2</sub>O<sub>3</sub> content. He examined the SEM micrographs and stated that the microstructures of the glass ceramic article was of vital significance in determining the mechanical and electrical properties thereof. In compositions contained less than about 5 wt% B<sub>2</sub>O<sub>3</sub>, the percentage of crystallinity can be as high as 65 % by volume but aspect ratio of the crystals was not great, perhaps averaging about 3-4. This resulted in a product exhibiting some machinability but with good mechanical strength and also there was only limited intrerlocking of the mica crystals. In composition contained greater than 5 wt% B<sub>2</sub>O<sub>3</sub>, he observed large interlocked platelets of mica crystals with a high aspect ratio and the texture resembled a house of cards microstructures that manifested the best properties. In this thesis, it was not possible to observe any distinct difference between the microstructures of the samples which contained 4wt% B<sub>2</sub>O<sub>3</sub> and 8wt% B<sub>2</sub>O<sub>3</sub>.



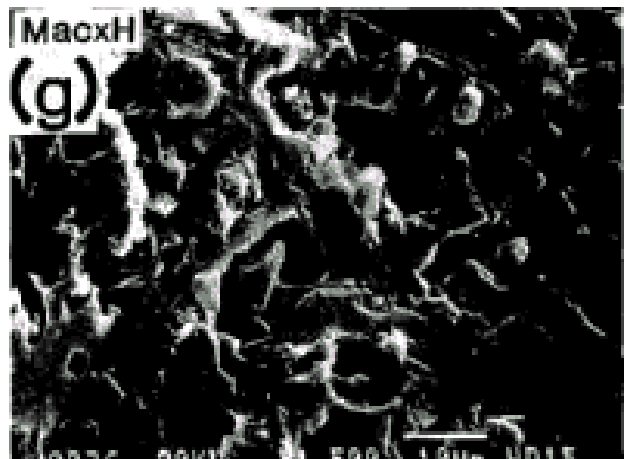
(a)



(b)



(c)



(d)

Figure 4.24 SEM micrograph of the samples given by Taira and Yamaki[26]

(a) Macor-M sample

(b) Photoveel sample

(c) Machinax sample 1

(d) Machinax sample 2

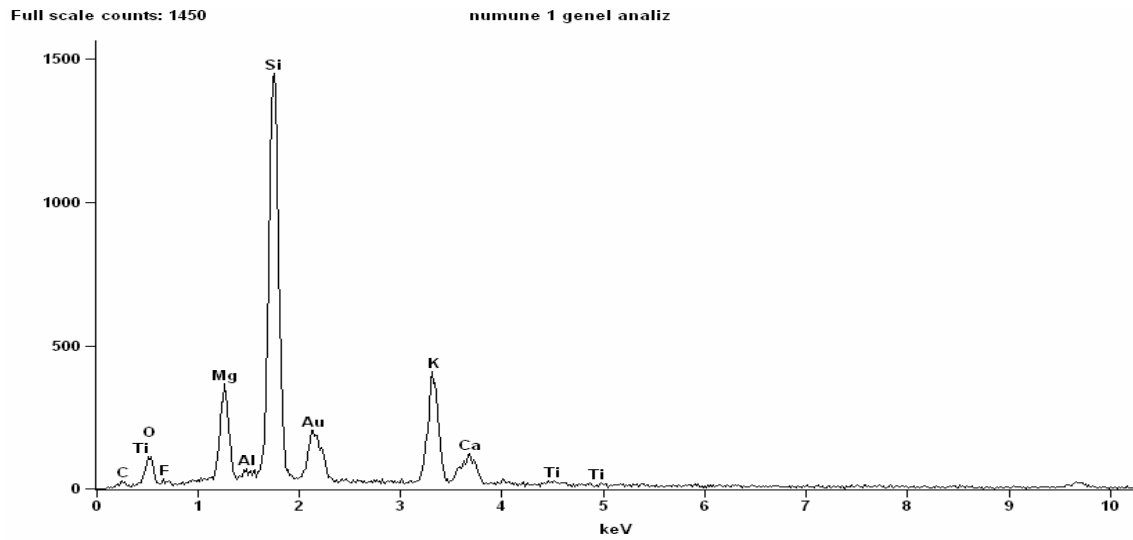
#### 4.2.4 Energy Dispersive X-Ray Analysis(EDX)

The samples containing 1, 4 and 8 wt% of  $B_2O_3$  exposed to different heat treatment were analyzed by EDX in order to make elemental analysis and hence to determine the chemical composition. The phases formed in the samples containing 4 and 8 wt%  $B_2O_3$  were analyzed in two cases; that is, the lid of the crucible was covered and was not covered during melting.

The EDX pattern and chemical analysis of the sample containing 1 wt%  $B_2O_3$  heat treated at 650 °C for nucleation and at 850 °C for growth were shown in Figure 4.25. As seen from the figure O, F, Mg, Al, Si, K, Ca, and Ti were detected. Although 1 wt% of  $B_2O_3$  was added to the batch of the sample, Boron was not detected by EDX due to the absence of the special apparatus of the EDX unit. The elements converted to their most stable oxide composition as MgO,  $Al_2O_3$ ,  $SiO_2$ ,  $K_2O$ , CaO, and  $TiO_2$ . Fluorine was kept in the elemental form which is believed to be present in the glass ceramic structure in the elemental form.

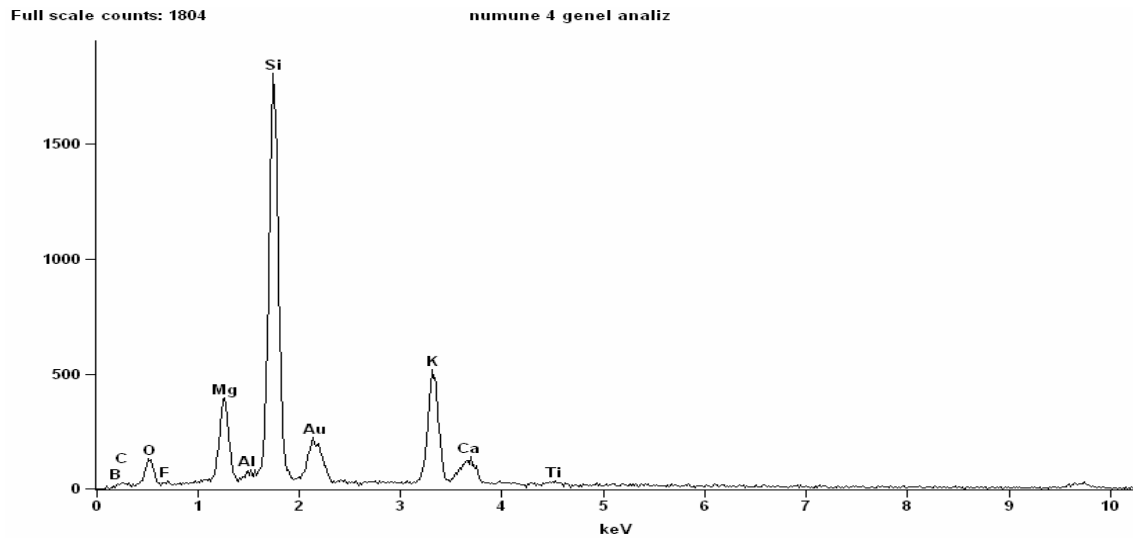
When the composition of the glass given in Figure 4.25 was compared with the composition of the batch given in Table 3.1; both compositions were more or less the same.  $SiO_2$  61.37 wt%, MgO 12.94 wt%,  $K_2O$  12.70 wt% and CaO 4.27 wt% content were slightly higher but  $Al_2O_3$  0.33 wt% and  $TiO_2$  0.92 wt% content were slightly lower than the original composition.

The EDX pattern and chemical analysis of the sample with the same composition but heat treated at 650 °C for nucleation and at 1000 °C for growth suggested that the same elements were detected as seen in Figure 4.26. However, the amounts of the elements and their corresponding oxides, was slightly different. The amount of the fluorine content decreased from 7.48 wt% to 4.53 wt%. As discussed in Section 4.2.2, higher crystallization temperatures caused more fluorine evaporation.



| <i>Element</i> | <i>Weight<br/>Conc %</i> | <i>Atom<br/>Conc %</i> | <i>Compnd<br/>Conc %</i> | <i>Formula</i>                 |
|----------------|--------------------------|------------------------|--------------------------|--------------------------------|
| <i>O</i>       | 41.71                    | 55.39                  | 0.00                     |                                |
| <i>F</i>       | 7.48                     | 8.37                   | 7.48                     | F                              |
| <i>Mg</i>      | 7.80                     | 6.82                   | 12.94                    | MgO                            |
| <i>Al</i>      | 0.17                     | 0.14                   | 0.33                     | Al <sub>2</sub> O <sub>3</sub> |
| <i>Si</i>      | 28.69                    | 21.70                  | 61.37                    | SiO <sub>2</sub>               |
| <i>K</i>       | 10.54                    | 5.73                   | 12.70                    | K <sub>2</sub> O               |
| <i>Ca</i>      | 3.05                     | 1.62                   | 4.27                     | CaO                            |
| <i>Ti</i>      | 0.55                     | 0.25                   | 0.92                     | TiO <sub>2</sub>               |

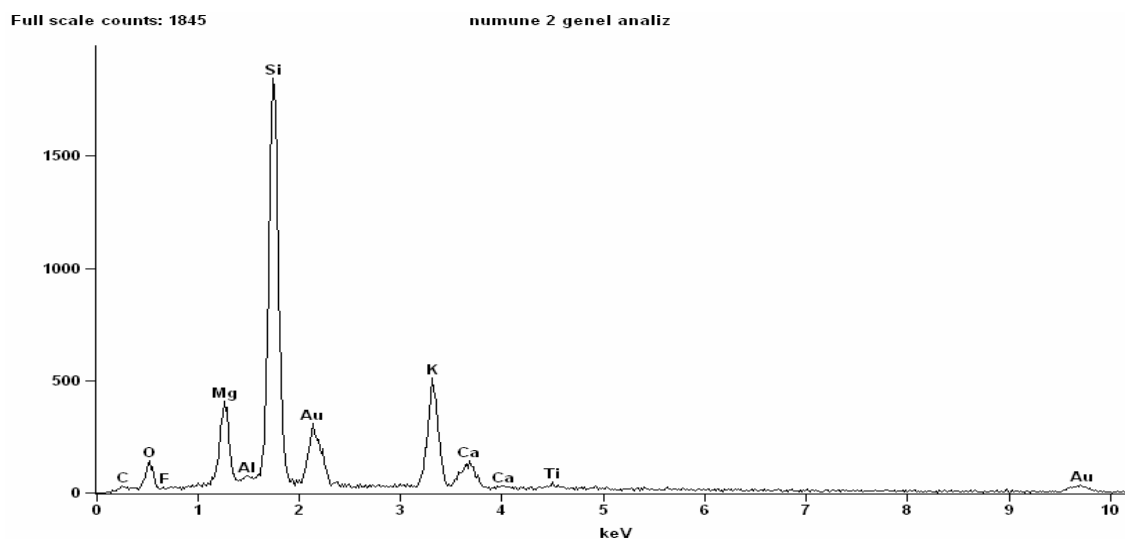
Figure 4.25 The EDX pattern and analysis of the sample containing 1 wt% B<sub>2</sub>O<sub>3</sub> heat treated at 650 °C for nucleation and at 850 °C for growth.



| <i>Element</i> | <i>Weight Conc %</i> | <i>Atom Conc %</i> | <i>Compnd Conc %</i> | <i>Formula</i>                 |
|----------------|----------------------|--------------------|----------------------|--------------------------------|
| <i>O</i>       | 42.74                | 57.17              | 0.00                 |                                |
| <i>F</i>       | 4.53                 | 5.10               | 4.53                 | F                              |
| <i>Mg</i>      | 7.87                 | 6.88               | 13.03                | MgO                            |
| <i>Al</i>      | 0.11                 | 0.09               | 0.20                 | Al <sub>2</sub> O <sub>3</sub> |
| <i>Si</i>      | 29.43                | 22.42              | 62.96                | SiO <sub>2</sub>               |
| <i>K</i>       | 11.98                | 6.56               | 14.44                | K <sub>2</sub> O               |
| <i>Ca</i>      | 2.67                 | 1.43               | 3.74                 | CaO                            |
| <i>Ti</i>      | 0.67                 | 0.30               | 1.11                 | TiO <sub>2</sub>               |

Figure 4.26 The EDX pattern and analysis of the sample containing 1 wt% B<sub>2</sub>O<sub>3</sub> heat treated at 650 °C for nucleation and at 1000 °C for growth.

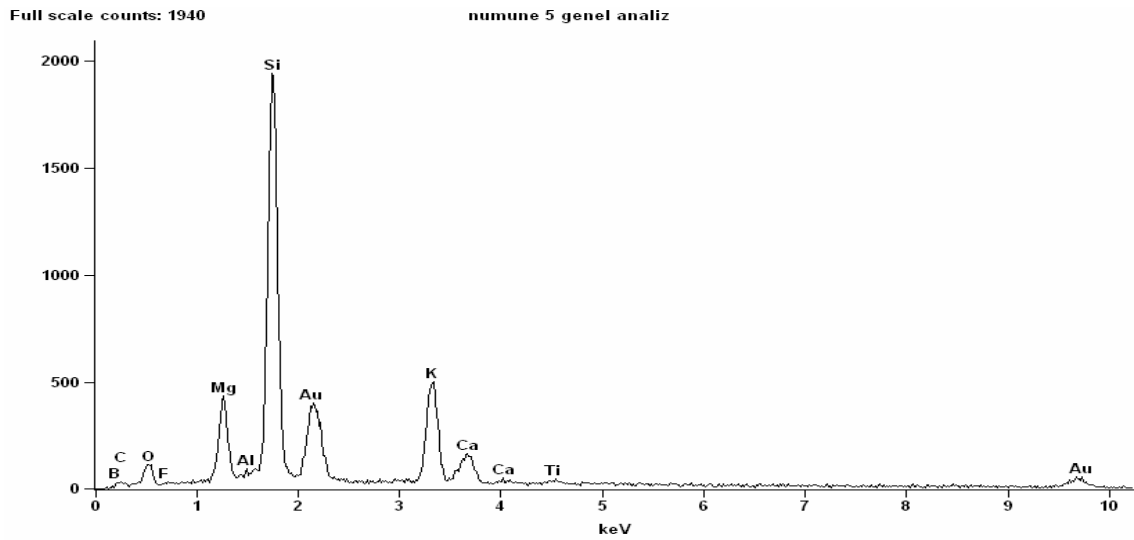
The EDX pattern and chemical analysis of the sample containing 4 wt% B<sub>2</sub>O<sub>3</sub> heat treated at 650 °C for nucleation and at 850 °C for growth were shown in Figure 4.27. Although the same elements were detected, fluorine content decreased to 2.00 wt%. Increasing B<sub>2</sub>O<sub>3</sub> content in the batch, caused a decrease in the fluorine content in the glass ceramic formed upon crystallization.



|           | <i>Weight<br/>Conc %</i> | <i>Atom<br/>Conc %</i> | <i>Compnd<br/>Conc %</i> | <i>Formula</i>                 |
|-----------|--------------------------|------------------------|--------------------------|--------------------------------|
| <i>O</i>  | 43.58                    | 58.69                  | 0.00                     |                                |
| <i>F</i>  | 2.00                     | 2.26                   | 2.00                     | F                              |
| <i>Mg</i> | 7.80                     | 6.89                   | 12.94                    | MgO                            |
| <i>Al</i> | 0.10                     | 0.08                   | 0.20                     | Al <sub>2</sub> O <sub>3</sub> |
| <i>Si</i> | 30.85                    | 23.59                  | 65.00                    | SiO <sub>2</sub>               |
| <i>K</i>  | 11.60                    | 6.37                   | 13.97                    | K <sub>2</sub> O               |
| <i>Ca</i> | 3.32                     | 1.78                   | 4.65                     | CaO                            |
| <i>Ti</i> | 0.75                     | 0.34                   | 1.25                     | TiO <sub>2</sub>               |

Figure 4.27 The EDX pattern and analysis of the sample containing 4 wt% B<sub>2</sub>O<sub>3</sub> heat treated at 650 °C for nucleation and at 850 °C for growth.

The EDX pattern and the chemical analysis of the sample with the same composition but heat treated at 650 °C for nucleation and at 1000 °C for growth were shown in Figure 4.28. Fluorine content was determined as 2.11 wt%. The change in fluorine content was not significant for the samples containing 4 wt% B<sub>2</sub>O<sub>3</sub> exposed to different crystallization temperatures.

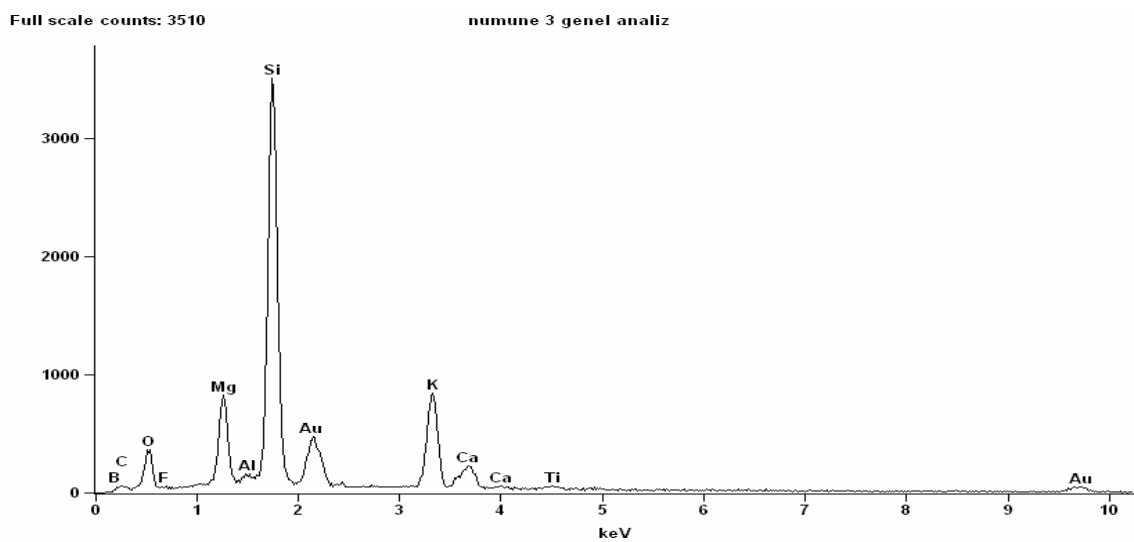


| <i>Element</i> | <i>Weight Conc %</i> | <i>Atom Conc %</i> | <i>Compnd Conc %</i> | <i>Formula</i>                 |
|----------------|----------------------|--------------------|----------------------|--------------------------------|
| <i>O</i>       | 42.64                | 57.99              | 0.00                 |                                |
| <i>F</i>       | 2.11                 | 2.38               | 2.11                 | F                              |
| <i>Mg</i>      | 7.57                 | 6.73               | 12.55                | MgO                            |
| <i>Al</i>      | 0.12                 | 0.10               | 0.21                 | Al <sub>2</sub> O <sub>3</sub> |
| <i>Si</i>      | 30.84                | 23.70              | 63.59                | SiO <sub>2</sub>               |
| <i>K</i>       | 11.96                | 6.60               | 14.41                | K <sub>2</sub> O               |
| <i>Ca</i>      | 3.99                 | 2.15               | 5.58                 | CaO                            |
| <i>Ti</i>      | 0.77                 | 0.35               | 1.28                 | TiO <sub>2</sub>               |

Figure 4.28 The EDX pattern and analysis of the sample containing 4 wt% B<sub>2</sub>O<sub>3</sub> heat treated at 650 °C for nucleation and at 1000 °C for growth.

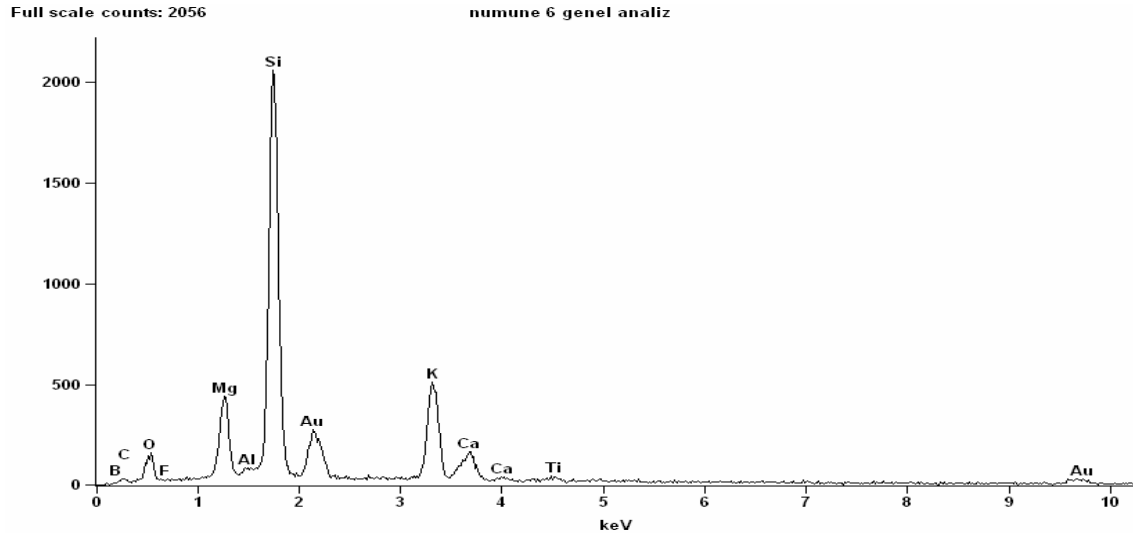
The EDX pattern and the chemical analysis of the sample containing 8 wt% B<sub>2</sub>O<sub>3</sub> heat treated at 650 °C for nucleation and at 850 °C for growth was shown in Figure 4.29. The same elements were detected. Fluorine content were 3.48 wt%.

The EDX pattern and chemical analysis of the sample with the same composition but heat treated at 650 °C for nucleation and at 1000 °C for growth were shown in Figure 4.30. Fluorine decreased almost by half when compared to the sample heat treated at 650 °C for nucleation and at 850 °C for growth.



| <i>Element</i> | <i>Weight<br/>Conc %</i> | <i>Atom<br/>Conc %</i> | <i>Compnd<br/>Conc %</i> | <i>Formula</i>                 |
|----------------|--------------------------|------------------------|--------------------------|--------------------------------|
| <i>O</i>       | 43.90                    | 58.34                  | 0.00                     |                                |
| <i>F</i>       | 3.48                     | 3.90                   | 3.48                     | F                              |
| <i>Mg</i>      | 8.18                     | 7.15                   | 13.56                    | MgO                            |
| <i>Al</i>      | 0.13                     | 0.11                   | 0.25                     | Al <sub>2</sub> O <sub>3</sub> |
| <i>Si</i>      | 30.54                    | 23.12                  | 65.34                    | SiO <sub>2</sub>               |
| <i>K</i>       | 10.68                    | 5.81                   | 12.87                    | K <sub>2</sub> O               |
| <i>Ca</i>      | 2.37                     | 1.26                   | 3.32                     | CaO                            |
| <i>Ti</i>      | 0.71                     | 0.31                   | 1.18                     | TiO <sub>2</sub>               |

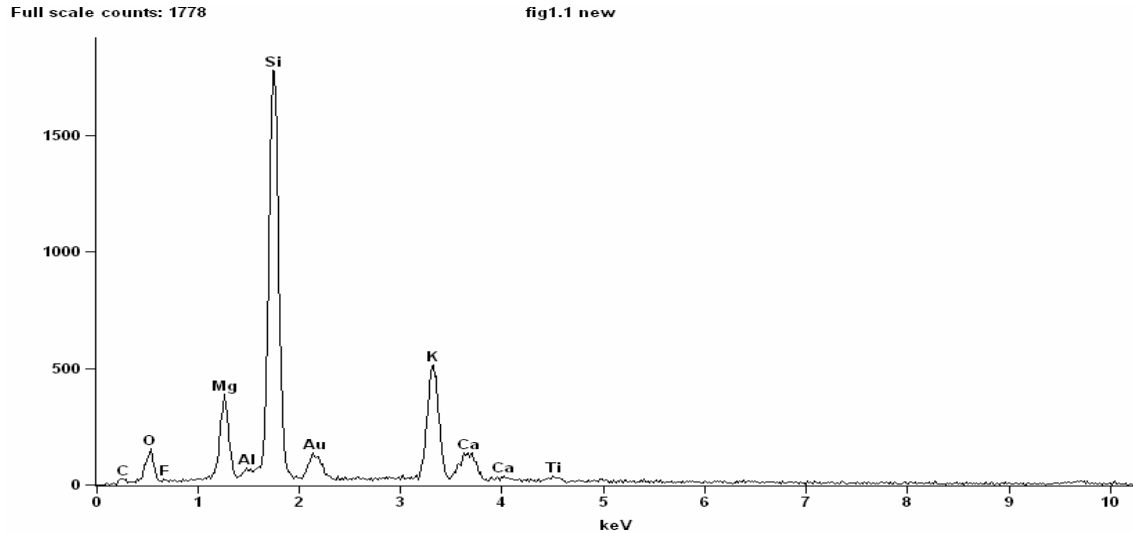
Figure 4.29 The EDX pattern and analysis of the sample containing 8 wt% B<sub>2</sub>O<sub>3</sub> heat treated at 650 °C for nucleation and at 850 °C for growth.



| <i>Element</i> | <i>Weight Conc %</i> | <i>Atom Conc %</i> | <i>Compnd Conc %</i> | <i>Formula</i>                 |
|----------------|----------------------|--------------------|----------------------|--------------------------------|
| <i>O</i>       | 44.14                | 59.15              | 0.00                 |                                |
| <i>F</i>       | 1.94                 | 2.19               | 1.94                 | F                              |
| <i>Mg</i>      | 7.98                 | 7.04               | 13.24                | MgO                            |
| <i>Al</i>      | 0.02                 | 0.02               | 0.04                 | Al <sub>2</sub> O <sub>3</sub> |
| <i>Si</i>      | 30.44                | 23.24              | 65.13                | SiO <sub>2</sub>               |
| <i>K</i>       | 11.29                | 6.19               | 13.60                | K <sub>2</sub> O               |
| <i>Ca</i>      | 3.44                 | 1.84               | 4.81                 | CaO                            |
| <i>Ti</i>      | 0.75                 | 0.33               | 1.24                 | TiO <sub>2</sub>               |

Figure 4.30 The EDX pattern and analysis of the sample containing 8 wt% B<sub>2</sub>O<sub>3</sub> heat treated at 650 °C for nucleation and at 1000 °C for growth.

The EDX pattern and the chemical analysis of the sample containing 4 wt% B<sub>2</sub>O<sub>3</sub> heat treated at 650 °C for nucleation and at 1000 °C for growth temperature were shown in Figure 4.31. The sample was obtained when the lid of the crucible was closed. As seen from the figures the same elements were detected. The amount of fluorine content was 4.22 wt%.

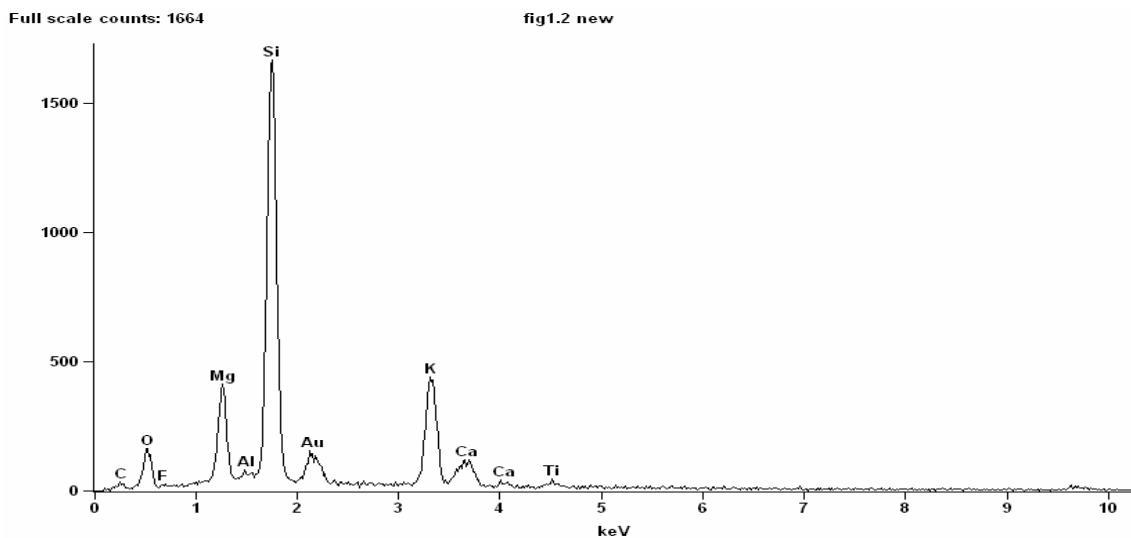


| <i>Element</i> | <i>Weight<br/>Conc %</i> | <i>Atom<br/>Conc %</i> | <i>Compnd<br/>Conc %</i> | <i>Formula</i>                 |
|----------------|--------------------------|------------------------|--------------------------|--------------------------------|
| <i>O</i>       | 41.20                    | 56.23                  | 0.00                     |                                |
| <i>F</i>       | 4.22                     | 4.82                   | 4.22                     | F                              |
| <i>Mg</i>      | 7.14                     | 6.37                   | 11.84                    | MgO                            |
| <i>Al</i>      | 0.02                     | 0.02                   | 0.04                     | Al <sub>2</sub> O <sub>3</sub> |
| <i>Si</i>      | 29.67                    | 22.89                  | 61.27                    | SiO <sub>2</sub>               |
| <i>K</i>       | 13.14                    | 7.28                   | 15.82                    | K <sub>2</sub> O               |
| <i>Ca</i>      | 3.63                     | 1.96                   | 5.08                     | CaO                            |
| <i>Ti</i>      | 0.97                     | 0.44                   | 1.62                     | TiO <sub>2</sub>               |

Figure 4.31 The EDX pattern and analysis of the sample containing 4 wt% B<sub>2</sub>O<sub>3</sub> heat treated at 650 °C for nucleation and at 1000 °C for growth. The sample was obtained when the lid of the crucible was closed.

The EDX pattern and the chemical analysis of the sample containing 8 wt% B<sub>2</sub>O<sub>3</sub> heat treated at 650 °C for nucleation and at 1000 °C for growth temperature were shown in Figure 4.32. The sample was obtained when the lid of the crucible was closed. The same elements were detected. The amount of the fluorine content in the samples were 4.04 wt%.

It is decidedly seen in Figure 4.29 and Figure 4.30 that the fluorine evaporation takes place in samples containing 8 wt% B<sub>2</sub>O<sub>3</sub> heat treated in both conditions when the lid of the crucible was opened during melting. When it was compared considering the fluorine evaporation, the samples obtained with lid of the crucible was closed during melting had twice much fluorine amount than the samples obtained with lid of the crucible was open as seen in Figure 4.31 and Figure 4.32.



| <i>Element</i> | <i>Weight Conc %</i> | <i>Atom Conc %</i> | <i>Compnd Conc %</i> | <i>Formula</i>                 |
|----------------|----------------------|--------------------|----------------------|--------------------------------|
| <i>O</i>       | 41.84                | 56.60              | 0.00                 |                                |
| <i>F</i>       | 4.04                 | 4.56               | 4.04                 | F                              |
| <i>Mg</i>      | 8.25                 | 7.29               | 13.67                | MgO                            |
| <i>Al</i>      | 0.24                 | 0.19               | 0.46                 | Al <sub>2</sub> O <sub>3</sub> |
| <i>Si</i>      | 29.79                | 22.79              | 61.72                | SiO <sub>2</sub>               |
| <i>K</i>       | 11.75                | 6.45               | 14.15                | K <sub>2</sub> O               |
| <i>Ca</i>      | 3.20                 | 1.71               | 4.48                 | CaO                            |
| <i>Ti</i>      | 0.89                 | 0.40               | 1.48                 | TiO <sub>2</sub>               |

Figure 4.32 The EDX pattern and analysis of the sample containing 8 wt% B<sub>2</sub>O<sub>3</sub> heat treated at 650 °C for nucleation and at 1000 °C for growth. Sample was obtained when the lid of the crucible was closed during melting.

The EDX analyses suggested that the fluorine content decreased when the crystallization temperature increased. Increasing the crystallization temperature caused the fluorine evaporation and decreased the fluorine content. For a given  $B_2O_3$  content, EDX analyses of the samples heat treated at 650 °C for nucleation and at 850 °C for growth had much fluorine content.

The EDX analysis revealed that as the  $B_2O_3$  content increased, the fluorine evaporation increased. There is no information in the literature about the fluorine evaporation with higher amount of  $B_2O_3$  content. The decrease in the amount of fluorine content with increasing  $B_2O_3$  content was attributed to the decrease of the nucleation and crystallization temperature and also glass transition temperature as discussed in Section 4.2.2.

The EDX analysis have revealed that the fluorine evaporation could be prevented by covering the top of the crucible. The fluorine content in the samples obtained when the top of the crucible was covered during melting was much higher than the fluorine content in the samples obtained when the top of the crucible was not covered during melting.

## CHAPTER 5

### CONCLUSIONS

1. Small amount of  $B_2O_3$  additions decreased the melting temperature of the mica glass ceramics.
2. According to the DTA analysis, increasing  $B_2O_3$  content in the samples decreased the glass transition and crystallization temperatures.
3. XRD analyses suggested that synthetic mica, fluorophlogopite, dehydroxylated muscovite, diopside, wollastonite and sinhalite crystals precipitated upon subjecting the glass to a suitable heat treatment. Sinhalite was observed to form when  $B_2O_3$  content was 4 wt % or higher.
4. SEM analysis revealed that, increasing  $B_2O_3$  content in the samples decreased the amount of crystallinity of the samples. Development of Diopside crystals resulted in the formation of pores in and around the grains.
5. Increasing  $B_2O_3$  content increased the opportunity of obtaining better microstructure such as longer and larger flakes of the mica crystals.
6. EDX analysis showed that fluorine content of the samples decreased due to the higher amount of fluorine evaporation when the growth temperature increased from 850 °C to 1000 °C. Also, increasing  $B_2O_3$  content of the sample caused higher amount of fluorine evaporation.

7. Covering of the top of the crucible with a lid during melting was advantageous in that it prevented the volatilization of fluorine whose evaporation was proved.

8. Microstructure of the mica glass ceramic produced in this study were comparable with that of commercially produced glass ceramics. Therefore, it may be an alternative to many commercial dental materials commonly used for dental applications.

### **RECOMMENDATIONS FOR FURTHER STUDIES**

1. Mechanical performances of the samples produced in this study, should be determined to see the effects of  $B_2O_3$  on mechanical properties.

2. Biocompatibility and machinability tests of the mica glass ceramics should be performed.

3. The effects of the diopside and sinhalite phases on the mica glass ceramics should be investigated in detail.

## REFERENCES

- [1] G. H. Beall, "Mica Glass Ceramics" US Patent Office, Patent Number : 3 689 293, Patent Date: September 5, (1972)
- [2] G. H. Beall, "Glass – Ceramics: Current Problems and Prospects for 2004" Journal of Non – crystalline Solids, Vol.73, (1985) pp: 413-419
- [3] P. F. James, "Glass – Ceramics: New Compositions and Uses" Journal of Non – crystalline Solids, Vol. 181, (1995) pp: 1-15
- [4] M. C. Weinberg, "Nucleation and Crystallization in Liquids and Glasses" , Ceramic Transactions, Vol. 30, (1992) pp: 34-39
- [5] M. S. Bapna and H. J. Mueller, "Study of Devitrification of Dicor Glass" Biomaterials, Vol. 17, (1996) pp: 2045-2052
- [6] L. Rounan, Z. Peinan, "Phlogopite-Based Glass Ceramics" Journal of Non – crystalline Solids, Vol. 84, (1986) pp: 600-604
- [7] T. Uno, T. Kasuga, S. Nakayama, and A. J. Ikushima, "Microstructure of Mica-Based Nanocomposite Glass-Ceramics" Journal of American Ceramic Society, Vol. 76, (1993) pp: 539-541
- [8] J. M. Tzeng, J. G. Duh, K. H. Chung, C. C. Chan, "Al<sub>2</sub>O<sub>3</sub> and ZrO<sub>2</sub> Modified Dental Glass Ceramics" Journal of Material Science, Vol. 28, (1992) pp.6127-6135

- [9]** T. Uno, T. Kasuga, K. Nakjima “High Strength Mica Containing Glass-Ceramics” Journal of American Ceramic Society, Vol. 74, (1991) pp:3139-3141
- [10]** G. H. Beall “Mica Glass-Ceramics” US Patent Office, Patent Number: 3 801 295, Patent Date: April 2, (1964)
- [11]** K. Kodaira, H. Fukuda, S. Shimada and T. Matsushita “Preparation and Characterization of Fluorophlogopite-Fluormuskovite Mica Glass-Ceramics” Material Research Bulletin, Vol. 19, (1984) pp: 1427-1432
- [12]** V. L. K. Lou and A. H. Heuer, “ Volatility Diagrams for Silica, Silicon Nitride, and Silicon Carbide and their Application to High Temperature Decomposition and Oxidation” Journal of American Ceramic Society, Vol. 73, (1990), pp: 2785-3128
- [13]** H. Der, “Production of Biocompatible Mica Glass Ceramics for Dental Applications” M.S. Thesis, Middle East Technical University, Ankara, Turkey, (1998)
- [14]** W. H. Kingery, D. R. Uhlman, H. K. Bowl, “Introduction to Ceramics” (1976), pp: 468, 555 – 561
- [15]** L. L. Hench and W. June “Introduction to Bioceramics” (1993) pp: 1 – 25; 41-75
- [16]** L. L. Hench, “Bioceramics, A Clinical Success”, American Ceramic Society Bulletin, Vol.77, July (1998), pp: 67-76
- [17]** L. L. Hench “Bioceramics: from Concept to Clinic” American Ceramic Society Bulletin, Vol. 72 (1993) pp:93-98

- [18]** T. Kokubo, "Bioactive Glass Ceramics: Properties & Applications", *Biomaterials*, Vol. 12, (1991), pp: 155-163
- [19]** T. Kokubo, "Surface Chemistry of Bioactive Glass Ceramics" *Journal of Non-crystalline Solids*, Vol. 120, (1990) pp:138-151
- [20]** A. R. Boccacini, "Short communication: Machinability and Brittleness of Glass Ceramics" *Journal of Materials Processing Technology*, Vol. 65, (1997) pp: 302- 304
- [21]** J. L. Xie, H. Feng, S. Wenhua, "Crystallization Properties of Phlogopite-based Machinable Glass Ceramic", *Journal of Material Science*, Vol. 37, (1996) pp:175-178
- [22]** H. H. K. Xu, D. T. Smith, S. Jahanmir, "Influence of Microstructure on indentation and Machining of Dental Glass-Ceramics" *Journal of Materials Research*, Vol. 11, (1996) pp: 2325-2337
- [23]** W. Vogel, "Glass Chemistry", 2<sup>nd</sup> Edition, Springer-Verlag, (1994)
- [24]** J. B. Park, "Biomaterials", 1979, Plenum Press, pp: 1-15, 226-231
- [25]** W. Vogel, W. Höland, and K. Nauman "Development of Machinable Bioactive Glass – Ceramics for Medical Uses", *Journal of Non-crystalline Solids*, Vol. 80, (1986) pp: 34-51
- [26]** P. W. McMillan, "The Crystallization of Glasses" *Journal of Non-crystalline Solids*, Vol. 52, (1982) pp: 67-76
- [27]** G. Fischman, A. Clare, and L. Hench, "Bioceramics: Materials and Applications", *Ceramic Transactions*, Published by American Ceramic Society, Vol.48, (1994) pp: 11-21, 35-41, 157-172

- [28]** T. Kokubo, S. Ito, S. Sakka, and T. Yamamuro, "Formation of the High Strength Bioactive Glass-Ceramics in The System MgO-CaO-SiO<sub>2</sub>-P<sub>2</sub>O<sub>5</sub>", Journal of Materials Science, Vol. 21, (1986) pp: 536-540
- [29]** W. Höland, P. Wange, K. Naumann, J. Vogel, G. Carl, C. Jana, and W. Götz "Control of Phase Formation Process in Glass Ceramics for Medicine and Technology" Journal of Non-crystalline Solids, Vol. 129, (1991) pp: 152-162
- [30]** X. Chen, L. Hench, D. Greenspan, J. Zhong, and X. Zhang,"Investigation on Phase Separation, Nucleation and Crystallization in Bioactive Glass-Ceramics Containing Fluorophlogopite and Fluorapatite",Ceramics International, Vol. 24, ( 1998) pp: 401-410
- [31]** S. N. Hoda, G. H. Beall, "Alkaline Earth Mica Glass Ceramics" Advances in Ceramics, Vol.4, pp: 287-300
- [32]** W. Höland, K. Naumann, H. G. Seiferth and W. Vogel, Z. Chemie 21 (1981), p.108
- [33]** W. Vogel, W. Höland and K. Naumann, Germany Patent Office Number: DDR-WP 223935 (1980)
- [34]** T. Ozawa "Kinetics of Non-Isothermal Crystallization", Polymer, Vol. 12, (1971) pp: 150-157
- [35]** F. Skyara, V. Sataya, "Kinetic Data from DTA measurement", Journal of Thermal Analysis, Vol.2, (1970) pp: 325-335
- [36]** J. A. Augis, J. E. Benneth, "Calculation of the Avrami Parameters for Heterogeneous Solid State Reactions Using a Modification of the

Kissinger Method”, Journal of Thermal Analysis, Vol.13, (1978) pp: 283-292

**[37]** A. Marotta, A. Buri, “Kinetics of Devitrification and Differential Thermal Analysis”, Thermochim Acta (1978) pp: 25: 155-160

**[38]** A. Marotta, A. Buri, F. Branda, S. Saiello, “Nucleation and Crystallization of  $\text{Li}_2\text{O}\cdot 2\text{SiO}_2$  Glass – A DTA Study”, In: Simons JH., Uhlmann Dr, Beall GH.,eds. “Nucleation and Crystallization in Glasses”, Advances in Ceramic, (Vol. 4), Columbus: The American Ceramic Society; (1982) pp: 146-152

**[39]** A. Bezak, E. Tkalcek, H. Ivankovic, M. Eres, “Determination of Kinetic Parameters for Nucleation and Growth from DTA data”, Thermochim Acta, (1993) pp: 221: 23-29

**[40]** J. Shyu, J. Wu, “Effect of  $\text{TiO}_2$  Addition on the Nucleation of Apatite in an  $\text{MgO-CaO-SiO}_2\text{-P}_2\text{O}_5$  Glass”, Journal of Materials Science Letters, Vol. 10, (1991) pp: 1056-1058

**[41]** S. Jahanmir, X. Dong, “Case Study: Wear Mechanism of a Dental Glass Ceramic Wear”, Vol. 181-183, (1995) pp: 821-825

**[42]** J. L. Xie, H. Feng, S. Wenhua, “Crystallization Properties of Phlogopite-based Machinable Glass Ceramic” Vol.37, (1996) pp: 175 – 178

**[43]** K. Cheng, J. Wan, K. Liang, “Effect of Fluorine Source on Crystallization of  $\text{R}_2\text{O-MgO-Al}_2\text{O}_3\text{-B}_2\text{O}_3\text{-SiO}_2\text{-F}$  (  $\text{R} = \text{K}^+, \text{Na}^+$  ) Glasses”, Journal of Materials Science and Engineering, Vol. A271, (1999) pp:167-171

- [44]** K. Cheng, J. Wan, K. Liang, "Crystallization of  $R_2O$ - $MgO$ - $Al_2O_3$ - $B_2O_3$ - $SiO_2$ - $F$  (  $R = K^+$  ,  $Na^+$  ) Glasses with Different Fluorine Source", Journal of Materials Letters, Vol. 47, (2001) pp:1-6
- [45]** J. E. Flannery, "Spontaneously Formed Flour Mica Glass Ceramics", US Patent Office, Patent Number: 3 985 534, Patent Date: October 12, (1976)
- [46]** W. Shi and P. F. James, in: Proceedings of 7<sup>th</sup> Conference on The Physics of Non-crystalline Solids, ed. L. D. Pye, W. C. Lacourse, H. J. Stevens (Society of Glass Technology, Taylor and Francis, London, 1992) p. 401
- [47]** W. Shi and P. F. James, "Crystallization and Properties of  $CaO$ - $P_2O_5$ - $B_2O_3$  glasses", Journal of Materials Science, Vol. 28, (1993), p. 469
- [48]** P. F. James and W. Shi, "Crystal Nucleation Kinetics in a  $40CaO$ - $40P_2O_5$ - $20B_2O_3$  Glass a Study of Heterogeneously Catalysed Crystallization", Journal of Materials Science, Vol. 28, (1993), p. 2260
- [49]** R. R. Tummala, "Ceramic and Glass-Ceramic Packaging in the 1990's", Journal of American Ceramic Society, Vol. 74, (1991), p. 895
- [50]** J. Black, "Systemic effect of Biomaterials" Biomaterials, Vol. 5, (1984), pp: 11-18
- [51]** D. G. Grossman "Tetra Silicic Mica Glass-Ceramics" US Patent Office Patent Number: 3 149 982, Patent Date: October 1, (1974)
- [52]** D. G. Grossman "Spontaneously Formed Machinable Glass-Ceramics" U.S. Patent Office, Patent Number: 4 239 520, Patent Date: December, (1980)

- [53]** H. Unuma, K. Miura, K. Kodeira, "Improvement of Mechanical Properties of Machinable Glass-Ceramics through Postmachining Heat Treatments" *Journal of American Ceramic Society*, Vol. 75, (1992) pp: 2300-2301
- [54]** M. L. Öveçoğlu, B. Kuban, H. Ozer, "Characterization and Crystallization Kinetics of a Diopside-Based Glass-Ceramic Developed from Glass Industry Raw Materials" *Journal of The European Ceramic Society*, Vol.17, (1997) pp: 975-962
- [55]** B. E. Yekta, S. H. Nia, P. Alizadeh, "The Effect of B<sub>2</sub>O<sub>3</sub>, PbO and P<sub>2</sub>O<sub>5</sub> on the Sintering and Machinability of Fluormica Glass-Ceramics" *Journal of The European Ceramic Society*, Vol. 25, (2005) pp:899-902
- [56]** K. Cheng, J. Wan, K. Liang, "Isothermal DTA Study on Crystallization of Mica Composition-Based Glass", *Journal of Non-Crystalline Solids*, Vol. 215, (1997) pp:134-139
- [57]** M. Taira and M. Yamaki, "Phase Constitution and Microstructural Characterization of Machinable Glass Ceramics", *British Ceramic Transactions*, Vol. 94, (1995) pp:109-112
- [58]** D. U. Tulyaganov, S. Agathopoulos, H. R. Fernandes, J. M. Ventura, J. M. Ferreira, "Preparation and Crystallization of Glasses in the System Tetrasilicic Mica-Fluorapatite-Diopside", *Journal of The European Ceramic Society*, Vol. 24, (2004) pp:3521-3528
- [59]** G. Werding, , K. Alsumady, W. Schreyer, O. Medenbach, "Low Pressure Synthesis, Physical Properties, Miscibility and Preliminary Stability of Sinhalite, MgAlBO<sub>4</sub>", *N. Jb. Miner. Abh.*, Vol. 141, (1981) pp : 201-216

- [60]** J. J. Capponi, J. Chevenas, J. C. Joubert, "Synthese Hydrothermale a Tres Haute Pression de Deux Borates de Type Olivine, MgAlBO<sub>4</sub>", Material Research Bulletin, Vol. 8, (1973) pp:275-282
- [61]** S. Krosse, P. Daniels, O. Medenbach, W. Schreyer, "Pseudosinhalite": Ein Neues Hochdruckborat. Z. Kristollogr., Vol.7, (1993) p.117
- [62]** S. Krosse, "Hochdrucksynthese, Stabilitat und Eigenschaften der Borsilikate Dravit und Kornerupin Sowie Darstellung und Stabilitatsverhalten eines neuen Mg-Al- borates", Unpublished Doctoral Thesis. Ruhr-Universitat Bochum, (1995) p. 120
- [63]** G. Werding, W. Schreyer, "Experimental Studies on Borosilicates and Selected Borates", Mineralogical Society of America. Rev. Mineral., Vol. 33, (1996) pp:117-163
- [64]** Grew, E.S., Cooper, M.A., Hawthorne, F.C., 1996. Prismaticine: Revalidation for Boron-Rich Compositions in the Kornerupine Group. Mineral. Mag. Vol.51, pp:695-708.
- [65]** A. W. A. El-Shennawi, E. M. A. Hamzawy, G. A. Khater, A. A. Omar, "Crystallization of Some Aluminosilicate Glasses", Ceramic Internationals, Vol. 27, (2000) pp:725-730
- [66]** S.S. Salama and H. Darwish, "Crystallization and Properties of Glasses Based on Diopside-Ca-Tschermak's-Fluorapatite System" Journal of The European Ceramic Society, Vol. 10, (2004) pp:1016-1025